# Co-expression of Bovine leukemia virus and Bovine foamy virus-derived miRNAs in naturally infected cattle

Petersen MI[1,2], Suarez Archilla G[3], Perez CV[1,2], Gonzalez DD[1,2], Trono KG[1,2], Mongini C[1,2], Jaworski JP[1,2], Carignano HA[1,2*].

## Affiliations

[1] Instituto de Virología e Innovaciones Tecnológicas, Instituto Nacional de Tecnología Agropecuaria - Consejo Nacional de Investigaciones Científicas y Técnicas, B1686 Hurlingham, Argentina.

[2] Consejo Nacional de Investigaciones Científicas y Técnicas, C1033AAJ Ciudad Autónoma de Buenos Aires, Argentina.

[3] Instituto de Investigación de la Cadena Láctea, Estación Experimental Agropecuaria Rafaela, Instituto Nacional de Tecnología Agropecuaria - Consejo Nacional de Investigaciones Científicas y Técnicas, S2300 Rafaela, Argentina.

[*]Address correspondence to Hugo A. Carignano, carignano.hugo@inta.gob.ar

## Abstract

Among the viruses that encode miRNAs and infect cattle such as Bovine leukemia virus (BLV), Bovine foamy virus (BFV) and Bovine herpesviruses (BoHV), BLV has gained attention due to the critical role that BLV-miRNAs may play in inducing lymphosarcoma in infected animals. BLV is highly prevalent in the Americas and negatively affects dairy herds, primarily due to restrictions on the commercialization of dairy products from infected animals and a decrease in milk production. Mixed infections involving BLV and BFV appear to be common in cattle. Considering the ability of foamy viruses to cross species barriers, preventing their presence within the food chain is essential. We identified the co-expression of seven BLV-derived miRNAs (blv-miR-B1-3p, blv-miR-B2-5p, blv-miR-B2-3p, blv-miR-B3-5p, blv-miR-B3-3p, blv-miR-B4-3p and blv-miR-B5-5p) and three BFV-derived (bfv-miR-BF1-5p, bfv-miR-BF1-3p, and bfv-miR-BF2-5p) in naturally BLV-infected cows. Besides, seven differentially expressed bovine miRNAs (bta-miR-375, bta-miR-133a, bta-miR-677, bta-miR-1, bta-miR-3613a, bta-miR-9-5p and bta-miR-95) were identified between cows with high BLV proviral load and uninfected counterparts (fold change > |1.5| and q-value < 0.05). A comprehensive functional analysis of protein-protein interaction networks for genes targeted by both viral and host-derived miRNAs highlighted key pathways implicated in tumorigenesis and immune response. Although BLV and BFV derived miRNAs target different genes, their functional convergence may reflect coordinated viral modulation of host cellular processes, raising important concerns regarding their potential influence on disease severity and the increased dissemination of BFV. These findings offer new perspectives for creating diagnostic and treatment approaches to manage viral persistence and tumorigenesis in cattle.

## Importance

The Bovine leukemia virus (BLV) and Bovine foamy virus (BFV) are retroviruses that encode miRNAs and infect cattle. While the role of BFV-derived miRNAs remains unclear, BLV-miRNAs have gained attention for their potential involvement in oncogenesis. Mixed BLV-BFV infections are common and given foamy viruses' potential to cross species barriers, it is essential to prevent their presence in the food chain. We reported the co-expression of three BFV-derived miRNAs and seven BLV-derived

miRNAs in naturally infected cattle. A functional analysis of the protein-protein interaction graph of genes potentially targeted by both viral and host-derived miRNAs revealed key metabolic pathways associated with tumorigenesis and immune response regulation. The co-expression of BLV and BFV miRNAs suggests a potential functional interactions that may influence disease progression and BFV dissemination. These findings offer opportunities for developing diagnostic and therapeutic strategies to control viral persistence and tumor development in cattle.

## Introduction

The study of virus-host interactions has traditionally focused on how viral proteins modulate host proteins to hijack cellular processes in favor of viral replication and pathogenesis (1) However, like their host cells, many viruses encode regulatory non-coding RNAs, including small RNAs such as microRNAs (miRNAs), which provide new capacities for regulating host gene expression to ensure successful viral infection (2; 3; 4; 5). miRNAs are enzymatically processed small RNAs, typically 19–24 nucleotides (nt) long, that fine-tune gene expression at the post-transcriptional level (6). The regulatory function of miRNAs is primarily mediated by the RNA-induced silencing complex (RISC), which facilitates base-pairing between the mature miRNA´s 2–7 nucleotide seed region and the 3' untranslated region (3'UTR) of the target messenger RNA (mRNA) (7; 8). The miRNA-mRNA interaction induces mRNA degradation by cellular endonucleases or translational repression (8; 9). It is estimated that miRNAs may regulate at least 60% of the human coding genome (10; 11).

Host-derived microRNAs (miRNAs) regulate viral infections by exhibiting a dual nature that can benefit either the virus or the host. For example, host miRNAs that directly target viral RNA often enhance the viral life cycle. Conversely, host miRNAs can exert an indirect negative effect on the virus by targeting mRNAs that encode essential host factors necessary for the viral cycle or for establishing immune responses and defense mechanisms (5; 12). Given their high versatility in fine-tuning gene expression and their small coding size, it is not surprising that viruses have evolved the ability to express their own miRNAs (13). Since the first report of miRNAs encoded by the Epstein-Barr virus (EBV) (14), miRNAs encoded by DNA viruses have proven to be the most abundant, particularly those expressed by the

Herpesviridae family. In contrast, RNA viruses that express miRNAs are far less common and are typically restricted to those with a DNA intermediate. Additionally, several miRNA-like molecules have been identified in both positive and negative-sense RNA viruses (3; 15; 16; 17; 18; 19; 20; 21; 22; 23; 24; 25; 26; 27; 28).

Usually, viral miRNAs follow the same biogenesis and effector pathways as host miRNAs. However, certain retroviruses, such as members of the Spumaretrovirinae subfamily (e.g., Simian foamy virus (SFV) and Bovine foamy virus (BFV)) and the Orthoretrovirinae subfamily (e.g., Bovine leukemia virus (BLV)), decouples miRNA transcription from genomic transcription by employing RNA polymerase III instead of RNA polymerase II (21, 22; 23). This mechanism likely prevents the auto-degradation of viral genomes mediated by endonucleases during miRNA biogenesis. (29; 30).

Generally, the functional role of viral miRNAs involves the downregulation of both viral and host proteins; however, upregulation would also occur—either indirectly through the modulation of gene that act as transcriptional repressors, or directly, as some miRNAs can function as transcriptional activators by binding to specific DNA sequences or interacting with factors that enhance gene expression (18; 31; 32). Collectively, these actions modulate gene expression to regulate the viral life cycle (e.g., promoting or inhibiting cell proliferation and apoptosis), evade the host immune response, and establish latent or persistent infections (4; 16; 33; 34; 35). This is particularly evident in retroviruses and herpesviruses, where viral protein expression is strongly restricted during latency. The production of a low-antigenicity regulatory molecule provides a significant advantage for viral persistence while evading host immune detection (13; 36).

Viruses that encode miRNAs and infect cattle include BLV (21), BFV (23), Bovine herpesvirus 1 (BoHV-1) (37), and Bovine herpesvirus 5 (BoHV-5) (38). BoHV-1 encodes at least ten miRNAs, two of which have been implicated in maintaining latency both *in vivo and in vitro* (39; 40). In contrast, the functional roles and target genes of the three BFV-derived miRNAs remain poorly understood (41). Among BLV-encoded miRNAs, blv-miR-B4-3p is the most extensevely studied. It shares a seed sequence with miR-29a, an oncomiR that targets tumor suppressors such as peroxidasin homolog (*PXDN*) and HMG-box transcription factor 1 (*HBP1*), as reported in murine tumor-induction studies (42; 43). *In vitro* reporter assays have demonstrated that blv-miR-B4-3p exerts a repressive effect on the expression of *HBP1* and

*PXDN*. However, a negative correlation between *blv-miR-B4-3p* and *HBP1* expression has been documented, while levels of *PXDN* remained unchanged in ovine primary tumor B cells (21; 44). Additionally, recent findings indicate that *PXDN* expression is significantly downregulated in naturally BLV-infected cattle expressing blv-miR-B4-3p when compared to their non-infected counterparts. Notably, miR-29a expression remains unaffected in both groups (45).

The BLV prevalence reaches up to 85% in North America at farms-level and over 80% in lactating cows of Argentina's main dairy region (46; 47; 48; 49). International trade restrictions of livestock products from affected herds impact negatively the economy (50), but greater losses stem from reduced milk production and earlier culling of asymptomatic BLV carriers compared to BLV-free herds (51; 52).

Mixed infections involving BLV and BFV appear to be common in cattle (53). Given the ability of foamy viruses (FVs) to cross species barriers and cause zoonotic infections in humans, their presence in the food chain may be a potential risk to both human and animal health. Furthermore, cattle infected with BLV are more susceptible to co-infections with BoHV-1 (54; 55; 56).

This study identified the expression of three BFV-derived miRNAs and seven BLV-derived miRNAs in naturally BLV-infected cattle through small RNA sequencing analysis. No miRNAs from BoHV-1/5 were found. Seven bovine miRNAs showed differential expression between cattle infected with BLV/BFV and those uninfected with BLV. A functional analysis of the protein-protein interaction network for genes potentially targeted by both viral and host-derived miRNAs revealed key metabolic pathways associated with tumorigenesis and immune response regulation.

## Methods

### Selection of Animals

BLV-infected and non-infected samples were obtained from a previously phenotyped population as described in Petersen et al. (2021) (57). Briefly, 129 adult Holstein cows (over 3 years old sharing the same lactation period) from a dairy farm in the central region of Argentina -where the average individual prevalence of BLV exceeds 80% (49)- were initially screened. Since antibody levels have been reported

to reflect proviral load (PVL) *in vivo* (49, 58), anti-BLV ELISA (see below) was assesed at −10 months (T1) and −5 months (T2) before final sampling; mean percentage of reactivity (PR) was 122.7 ± 34.8 at T1 and 146.3 ± 55.6 at T2. Animals in the highest PR quartile (Q) (Q4: T1 = 148.6–178.6%, T2 = 194.4–239.6%) and those testing negative at both times were selected for further proviral load (PVL) quantification via qPCR (details provided later) at −3 months (T3) and at the time of sampling (T4). Based on the consistency of PVL results, four cows with persistently high PVL (HPVL) and three cows with consistently negative qPCR results were ultimately selected for small RNA sequencing. All sample collection and handling procedures adhere to the recommendations and guidelines of the Institutional Committee for the Care and Use of Experimental Animals at the Instituto Nacional de Tecnología Agropecuaria.

**Isolation of Peripheral Blood Mononuclear Cells (PBMCs)**

Fresh blood samples from animals were collected via jugular venipuncture and supplemented with EDTA (225 µM). Peripheral blood mononuclear cells (PBMCs) were isolated on the same day of collection using Ficoll-Paque Plus (GE Healthcare, Uppsala, Sweden) density gradient centrifugation, following the manufacturer's protocol. The plasma fraction was kept for anti-BLV ELISA serology. After isolation, PBMCs were preserved in RNAlater solution (Ambion, Austin, TX) and stored at −80°C until further use.

**Serology**

The anti-BLV ELISA assay, as described by Trono et al. (2001) (59), was employed to identify BLV-infected animals. The whole BLV viral particle served as the antigen for detecting plasma anti-BLV antibodies in each sample. Briefly, a sample-to-positive (S/P) ratio, referred to as the percentage of reactivity (PR), was calculated using the following formula: $S/P = [(OD_{Sample} - OD_{WS-}) / (OD_{WS+1/7} - OD_{WS-})] \times 100$, where OD refers to optical density, WS- indicates the negative serum, and WS+1/7 is the international standard weak positive control serum (diluted 1:7 in negative serum). Samples with a PR greater than 25% were considered positive (BLV(+)), while those below were regarded as negative (BLV(-)).

**BLV proviral load (PVL) Quantification**

Genomic DNA was extracted from PBMCs using the High Pure PCR Template Preparation Kit (Roche, Penzberg, Germany) following the manufacturer's instructions. The quality and concentration of genomic DNA from whole blood samples, extracted with the Blood Genomic DNA AxyPrep™ kit (Axygen Biosciences, Union City, USA), were assessed using a microvolume spectrophotometer (NanoDrop™ Technologies, Inc., Wilmington, USA).

A BLV POL gene-based PVL qPCR assay based on the SYBR Green dye detection system was conducted as described by Petersen et al. (2018) (60). Each 25 µL qPCR reaction contained Fast Start Universal SYBR Green Master Mix (2×; Roche), forward and reverse primers (800 nM; BLVpol_5f:5′-CCTCAATTCCCTTTAAACTA-3′ and BLVpol_3r:5′-GTACCGGGAAGACTGGATTA-3′; Thermo Fisher Scientific), and 200 ng of genomic DNA template. Amplification and detection were carried out using a Step One Plus system (Applied Biosystems, Foster City, CA). The specificity of each BLV-positive reaction was confirmed by melting temperature dissociation curve (Tm) analysis. Based on the assumption of a low natural infection rate (1% of BLV-infected cells in the peripheral blood), PVL values below 1,500 copies/µg of total DNA were classified as low, while values above this threshold were classified as high (61).

**Small RNA Sequencing**

Total RNA was extracted from PBMCs using the miRNeasy kit (Qiagen, Hilden, Germany) according to the manufacturer's protocol. RNA quality (integrity) and concentration were assessed via digital electrophoresis on an Agilent 2200 TapeStation system (Agilent Technologies, Santa Clara, US).

The QIAseq miRNA Library Kit (Qiagen, Hilden, Germany) was used for miRNA sequencing library construction, which integrates Unique Molecular Indices (UMIs) tags into the adapters during the cDNA synthesis step. These UMI tags help to mitigate PCR amplification biases and sequencing artifacts by allowing identification and collapsing reads with the same amplification origin. A specific 8-nt barcode was assigned to each sample for multiplexing. The multiplexed libraries were pooled to an equal molar concentration and processed in a NovaSeq run (Illumina, San Diego, US) with a 75x50 bp configuration (300–400 million reads pairs per lane).

**Small RNA sequencing reads processing and deduplication**

The quality control of sequencing reads was performed sequentially to ensure reliable reads for unbiased miRNome identification and quantification. The 12-nt UMI pattern was extracted from each read using the umi_tools v1.1.6 software (62). Forward (Fw) and reverse (Rv) reads were processed independently before collapsing. Reads with low quality (quality cutoff < 30), a minimum length < 16 nt, the presence of ambiguous bases (N) or adapter sequences were removed using Cutadapt v5.0 (63). Singleton reads resulting were discarded, and only paired Fw and Rv reads were considered. Forward read sequences were aligned to the Rv-complement and merged into a single consensus read using BBMap v25.85 (64) with a minimum insert size of 16 nt and a minimum overlap of 18 nt. After merging, Qiagen-specific adapter sequences were removed using Cutadapt v5.0 (63).

A stringent mapping strategy was employed for read deduplication using Bowtie2 v2.5.4 (65). Reads were aligned to the bovine reference genome ARS-UCD1.2 (acc. GCF_002263795.1) and to viral genomes encoding miRNAs that infect cattle, including BLV (acc. NC_001414.1), BFV (acc. NC_001831.1), BoHV-1 (acc. NC_063268.1) and BoHV-5 (acc. NC_005261.3). No mismatches were allowed in the first 18 bases of the read (left end). After alignment to the reference sequences, reads were deduplicated based on their mapping coordinates and the previously extracted UMI tags using UMICollapse v1.0.0 (66).

**miRNAs identification and quantification**

Deduplicated reads were mapped to the reference precursor miRNA sequences for bovine, BLV, BFV, BoHV-1 and BoHV-5 obtained from miRBase v22.1 (67). Mature miRNA expression was quantified using miRDeep2 v0.1.3 (68) with default parameters, generating a count matrix of miRNA expression for each sample.

**Differential miRNA Expression analysis**

The raw count matrix for all samples was analyzed using DESeq2 v1.44.0 (69) to assess differential miRNA expression between BLV-infected and non-infected animals. Based on miRNA expression profiles, an exploratory analysis of variation patterns between infected and non-infected animals was performed using principal component analysis (PCA). To ensure homoskedasticity of the data, raw

miRNA counts were transformed using the Variance Stabilizing Transformation (VST) method implemented in DESeq2 v1.44.0. Pairwise distances between samples were calculated based on the root-mean-square deviation of miRNA expression levels.

To test for differential miRNA expression, the DESeq2 model adjusts miRNA counts by accounting for sample-specific differences, such as library size, sequencing composition, and miRNA-specific biases, using negative binomial models. Under the null hypothesis, the model assumes that a miRNA has the same mean expression across the two conditions (BLV(-) and BLV(+) groups). The statistical significance of the $Log_2$ fold change ($Log_2FC$) between conditions was assessed using the Wald test. Correction for multiple comparisons was performed using the Benjamini-Hochberg false discovery rate (BH-FDR) method (70). The miRNAs with BH-FDR-adjusted p-values (q) < 0.05 and a $Log_2FC > |1.5|$ were considered statistically significant. The PCA and Volcano plots were performed under the R environment (71).

**miRNAs gene target prediction**

Significant differentially expressed bovine and viral-derived miRNAs between BLV(+) and non-infected cows were used to predict potential bovine gene targets *in silico* (miRNA:mRNA interactions) using miRanda v3.3 (72), PITA v6.0 (73), and RNAhybrid v2.1.1 (74), with default parameters. The analysis utilized 3´-UTR sequences of 21,400 bovine genes from the ARS-UCD1.2 annotation (75). Each gene target prediction algorithm employed a distinct strategy: miRanda relied on seed-site alignment and the thermodynamic stability of RNA-RNA duplexes; PITA incorporated target-site accessibility; and RNAhybrid uses the minimum free energy of hybridization between miRNA-mRNA sequences. Predicted targets were filtered using the following threshold: a score of ≥140 and free energy ≤−20 kcal/mol (miRanda) and free energy ≤−20 kcal/mol (PITA and RNAhybrid). Only gene targets predicted by all three tools (consensus gene targets) were retained for downstream analysis

**Gene ontology and graph-based pathway analysis of miRNA target genes**

The functional annotation of the potential target genes was carried out using STRINGdb (76) with Gene Ontology (GO) terms and Kyoto Encyclopedia of Genes and Genomes (KEGG) pathways (77). Next, a protein-protein interaction (PPI) network of the identified target genes was constructed using STRINGdb.

This platform integrates curated and predicted interactions from multiple sources, including experimental evidence, computational predictions, scientific literature, co-expression data and primary public databases. Highly interconnected protein clusters within the network were identified using the Markov Cluster Algorithm (MCL) with default parameters (inflation parameter = 2.5). Only clusters with more than 15 nodes (genes) were considered. GO terms and KEGG pathways overrepresentation analysis was performed on the identified clusters using Fisher's exact test based on the hypergeometric distribution, using a term similarity threshold > 0.7 (78). Wordclouds plots of significant GO terms grouped by semantic similarity were obtained using the rrvgo package with default parameters (79). A GO term category–gene target graph was generated to visualize the connections between significantly enriched GO terms and their associated genes using the R graphical environment (71).

## Results

In this study, four animals consistently exhibited both high antibody reactivity across all sampling times (IND_5671 = 178.6 ± 28.4; IND_5841 = 191.3 ± 32.8; IND_6021 = 169.8 ± 42.7 and IND_6097 = 183.2 ± 25.4) and high proviral loads at T-3 and T0 (average proviral load: IND_5671 = 63,148.0; IND_5841 = 44,234.3; IND_6021 = 52,902.4 and IND_6097 = 91,255.4). These cows were classified as BLV(+). In contrast, three animals that consistently tested negative for both anti-BLV ELISA and qPCR were classified as BLV(-).

Total RNA quality was confirmed (RIN 7.8–9.6), and small RNA libraries were prepared using UMI-tagged adapters. High-quality, non-redundant reads were obtained through a multi-step processing pipeline. A descriptive characterization of each sample, the number of sequencing reads before and after quality control; merging and deduplication; and mapping statistics are summarized in Table 1.

Demultiplexed reads were mapped to the reference miRNA sequences of bovine, BLV, BFV, BoHV-1 and BoHV-5 (n = 1060) to identify and quantify the miRNAs present in each sample. On average, 351 miRNAs (with mapped reads ≥ 5) derived from both bovine and viral sources were identified and quantified across all samples (Supp. Table S1). A multivariate analysis of sample distances based on the normalized miRNA expression matrix revealed that BLV(-) samples clustered together, forming a distinct

group separate from BLV(+) samples. PC1 explains 62% of the variance in the expression matrix, while PC2 accounts for 17% (Figure 1).

In the BLV(+) group, a total of 10 viral-derived miRNAs were consistently expressed, including 7 from BLV: blv-miR-B1-3p (avgexp = 27,681.1), blv-miR-B2-5p (avgexp = 59,058.0), blv-miR-B2-3p (avgexp = 112.5), blv-miR-B3-5p (avgexp = 309.6), blv-miR-B3-3p (avgexp = 49,312.2), blv-miR-B4-3p (avgexp = 65.1), and blv-miR-B5-5p (avgexp = 951.7). Additionally, 3 BFV-derived miRNAs were identified: *bfv*-miR-BF1-5p (avgexp = 6,844.7), bfv-miR-BF1-3p (avgexp = 8,257.3), and bfv-miR-BF2-5p (avgexp = 14,920.6). In contrast, viral-derived miRNAs expression was low (avgexp < 30.0) or undetectable in the BLV(-) group, except for blv-miR-B2-5p (avgexp = 67.4) and blv-miR-B3-3p (avgexp = 49.8) (Table 2).

The mapping of all reads from BLV(-) samples to the bovine reference genome (acc. ARS-UCD1.2) showed that only 716 out of 14,378,553 reads failed to align, indicating that nearly all reads were derived from bovine small RNAs. Besides, the number of reads aligned to the BLV (acc. NC_001414.1) and BFV (acc. NC_001831.1) reference genomes from BLV(-) cows were only 600 and 141 reads, respectively (Table 1). Moreover, the alignment of the same reads dataset to the identified BLV- and BFV- miRNAs resulted in 642 reads with at least one aligment. Among these, only six reads also map to the bovine reference genome, and none aligned any other known miRNA from any organism in the miRBase database (n = 48,871 mature miRNAs). The Supp. Figure S2 shows the coverage of all reads from BLV(+) and BLV(-) cows across the reference genomes of BLV and BFV, emphasizing that detectable read coverage is restricted to known miRNA regions for both viral genomes.

Differential expression analysis of host miRNAs, identified a total of seven bovine miRNAs (bta) with a fold change (FC) > |1.5| and a q-value < 0.05 as differentially expressed (BTA-miRNAs-DE) between the BLV(+) and BLV(-) groups: bta-miR-375, bta-miR-133a, bta-miR-677, bta-miR-1, bta-miR-3613a, bta-miR-9-5p, and bta-miR-95 (Figure 2; Supp. Table S2). In Supp. Figure S3, a heatmap was generated to visualize the expression of miRNAs in BLV(+) and BLV(-) cows. A hierarchical clustering was applied to both dimensions to show groups of samples with similar expression profiles, as well as clusters of miRNAs with coordinated expression patterns.

To evaluate the potential functional impact of the seven differentially expressed BTA-miRNAs and the ten viral-derived miRNAs, a target gene prediction analysis was performed. A total of 1,518 genes were

identified as putative targets, based on the consensus of three independent prediction tools. Among these, 281, 977, and 260 genes were exclusively targeted by BTA-miRNAs-DE, BLV-miRNAs, and BFV-miRNAs, respectively (Supp. Table S3). No overlap was observed among the predicted target. Then, functional annotation of the 1,518 potential target genes was conducted using Gene Ontology (GO) terms and metabolic pathways, revealing 91 significantly overrepresented GO biological process (BP) terms, 10 GO molecular function (MF) terms and 30 GO cellular component (CC) terms. The word cloud visualizations for the enriched GO terms in the GO BP and GO MF categories are shown in Figure 3, the most frequent occurring words for the overrepresented processes and functions included "Regulation", "Process", "Response", "Binding", "Activity", among others. The overrepresentation analysis of KEGG and Reactome metabolic pathways revealed four significant terms: "*Ras signaling pathway*" (bta04014, q = 0.04), "*Pathways in cancer*" (bta05200, q = 0.02), "*Oxytocin signaling pathway*" (bta04921, q = 0.024), and "*Cushing syndrome*" (bta04934, q = 0.04). Additionally, the terms "*Signal Transduction*" (BTA-162582, q = 0.0002) and "*Metabolism*" (BTA-1430728, q = 0.01) were significant in Reactome pathways analysis (Supp. Table S4).

A protein-protein interaction (PPI) network was developed, comprising 1,518 nodes (genes) and 6,075 edges (interactions) (Supp. Figure S2). From this network, three highly interconnected protein clusters (C1, C2, and C3) were identified (PPI p-value < $1.0e^{-16}$), which potentially represent hubs of specialized biological function (Figure 4). Functional overrepresentation analysis for these clusters revealed key cellular processes involved in immune response modulation, cell signaling, and mechanisms related to cancer development (Supp. Table S4). Interestingly, despite the lack of overlap among target genes of BTA-, BLV-, and BFV-derived miRNAs, their predicted functions converge on interconnected hubs, indicating potential interplay at the pathway level. The enrichment graph plot depicts the interconnections among the top 15 enriched BP GO terms per cluster, highlighting functional overlap through target genes (Figure 5).

For example, significantly overrepresented GO BP terms for C1 (q < 0.05), included "*Cytokine-mediated signaling pathway*", "*Signal transduction*", "*Positive regulation of leukocyte chemotaxis*", "*Positive regulation of immune system process*", "*Regulation of leukocyte proliferation*", "*Regulation of cell adhesion*", "*Myeloid leukocyte migration*", "*Positive regulation of T cell activation*", "*Regulation of*

*leukocyte apoptotic process*", "*Regulation of interferon-gamma production*", amog others, focusing especially on processes related to immune activation, cytokine production, and immune regulation. For C2, key terms represent biological processes primarily tied to cell growth, development, and tissue morphogenesis, such as "*Transmembrane receptor protein tyrosine kinase signaling pathway*", "*Vascular endothelial growth factor signaling pathway*", "*ERBB2-EGFR signaling pathway*", "*Positive regulation of MAP kinase activity*", "*Hemopoiesis*", "*Negative regulation of apoptotic process*", "*Anatomical structure morphogenesis*", "*Positive regulation of epithelial cell proliferation*", "*Positive regulation of mast cell chemotaxis*", among others.

In C3, the terms are mostly associated with epigenetic control and transcriptional regulation through chromatin modification, including "*Histone deacetylation*", "*Histone modification*", "*Chromatin remodeling*", "*Negative regulation of transcription by RNA polymerase II*", "*Chromosome organization*", "*Regulation of apoptotic signaling pathway*", among others.

Significantly enriched KEGG and Reactome pathways for clusters included, C1: "*Cytokine-cytokine receptor interaction*" (bta04060, q-value = $8.40e^{-22}$), "*Viral protein interaction with cytokine and cytokine receptor*" (bta04061, q-value = $1.02e^{-16}$), "*Cytokine Signaling in Immune system*" (BTA-1280215, q-value = $1.09e^{-06}$), "*Chemokine receptors bind chemokines*" (BTA-380108, q-value = $1.10e^{-06}$), "*Interleukin-21 signaling*" (BTA-9020958 q-value = 0.0057), "*IL-6-type cytokine receptor ligand interactions*" (BTA-6788467, q-value = 0.0105); C2: "*MAPK signaling pathway*" (bta0401, q-value = $3.50e^{-10}$), "*Regulation of actin cytoskeleton*" (bta04810, q-value = 0.0014), "*HIF-1 signaling pathway*" (bta04066, q-value = 0.0029), "*Signaling by Receptor Tyrosine Kinases*" (BTA-9006934, q-value = $3.13e^{-16}$), "*PI5P, PP2A and IER3 Regulate PI3K/AKT Signaling*" (BTA-6811558, q-value = $1.62e^{-09}$), "*PI3K Cascade*" (BTA-109704, q-value = 0.0034), "*Regulation of KIT signaling*" (BTA-1433559, q-value = 0.0058); and C3: "*Regulation of TP53 Activity through Acetylation*" (BTA-6804758, q-value = $2.85e^{-08}$), "*RNA Polymerase I Transcription Initiation*" (BTA-73762, q-value = $1.02e^{-07}$), "*Gene expression (Transcription)*" (BTA-74160, q-value = $3.05e^{-05}$), "*Chromatin modifying enzymes*" (BTA-3247509, q-value = $4.15e-^{05}$), "*Regulation of PTEN gene transcription*" (BTA-8943724, q-value = 0.00052).

## Discussion

In this study, we performed a comprehensive characterization of circulating miRNAs in the peripheral blood of naturally BLV-infected and non-infected cattle. Notably, all BLV-infected cows included in the analysis consistently exhibited HPVL levels across time points; a condition previously associated with BLV pathogenesis progression (80; 81) and increased risk of viral transmission within herds (82). Following the identification of BLV-miRNAs in persistently infected cell lines (21), their expression was assessed using next-generation sequencing for complete miRNA profiling and RT-qPCR to test the expression of candidate miRNAs. BLV-miRNAs were identified in primary leukemic B-cells and B-cell lymphomas isolated from BLV-infected ovine/bovine tumors (44), experimentally infected cattle (83), and naturally BLV-infected cattle (45; 84; 85).

On the other hand, BFV-miRNAs have been identified in both persistently and recently infected MDBK cells, as well as in BFV experimentally challenged cattle (23). However, to our knowledge, this is the first report of the co-expression of miRNAs derived from two distinct viruses (BLV and BFV) in naturally infected cattle. We identified and quantified seven BLV-derived and three BFV-derived miRNAs. No miRNAs from BoHV-1 and -5 were detected.

Coinfections of BLV and BFV are prevalent among cattle (53), akin to the occurrences in cats infected with Feline foamy virus (FFV) and Feline leukemia virus (FeLV) (86), as well as in baboons with Simian foamy virus (SFV) and Simian T-cell leukemia virus (STLV) (87). While BFV infections in cattle are generally regarded as mild and asymptomatic (23; 53), there is evidence to suggest that co-infections with BFV and BLV could amplify pathogenicity and impair the bovine immune system, thereby aiding in the transmission and spread of BFV (53; 88; 89; 90). Infectious BFV has been extracted from raw milk, and considering that foamy viruses can cross species barriers, there is rising concern over the zoonotic potential of BFV in humans (91; 92). Moreover, increased pathogenic effects have been noted in mixed infections of macaques with SFV and Simian immunodeficiency virus (SIV) (93), as well as in cats coinfected with Feline immunodeficiency Virus (FIV) and FFV or FeLV and FFV (86; 94).

The seven miRNAs derived from BLV comprised no more than 8% of the total miRNA sequencing reads in all analyzed samples (data not provided), consistent with the expression levels reported by Casas et al. (2020) (85) for natural BLV infections. In contrast, Rosewick et al. (2013) (44) found that all ten mature BLV-derived miRNAs accounted for about 40% of total miRNAs present in B-cell lymphomas from sheep infected with BLV. Similarly, Ochiai et al. (2021) (95) noted that BLV-derived miRNAs made up 38% of total miRNAs in Japanese black cattle diagnosed with enzootic bovine leukosis (B-cell lymphoma). Additionally, Kincaid et al. (2012) (21) reported that BLV miRNAs were found in greater quantities than cellular miRNAs in the BL3.1 cell line persistently infected with BLV. Although the relative expression levels of individual BLV miRNAs differ across studies, blv-miR-B4-5p and blv-miR-B5-3p appear to be either weakly expressed or undetectable. The dominant BLV-miRNA may change depending on the disease stage or phase of infection analyzed. Overall, these findings suggest that BLV miRNAs are highly expressed in *ex vivo* cell cultures, persistently infected cell lines, primary B-cell tumors, and cattle affected by enzootic bovine leukosis. In cattle with subclinically BLV-infections, their expression levels might vary based on several factors, including the infection route (natural or experimental) and the animal's age (whether calf or adult cow), among other factors (21; 44; 83; 84; 85; 95). Conversely, the other BLV transcripts show little to no expression *in vivo*, highlighting the essential function of BLV miRNAs in viral persistence (96; 97).

Likewise, three BFV-derived miRNAs (bfv-miR-BF1-5p, bfv-miR-BF1-3p, and bfv-miR-BF2-5p) have been identified in MDBK cells that are persistently and recently infected with BFV, showing higher expression levels during persistent infections. Furthermore, two BFV-miRNAs were found in the peripheral blood leukocytes of cattle experimentally infected with BFV, utilizing a qPCR assay (23). This research is the first to document the expression of these three BFV-derived miRNAs in natural setting infections.

A previous study compared BLV seropositive and seronegative cattle but without testing for BLV genomic material (85). The detection of BLV-miRNAs in seronegative cows suggests a previous exposure to the virus, likely resulting in an inadequate immune response that did not generate a positive result in the anti-BLV ELISA test. However, a longitudinal analysis of seroconversion was not performed. This study found that all ten virus-derived miRNAs were consistently and highly expressed in the BLV(+)

group, whereas only a few showed weak expression in the BLV(-) group. Although undetected infections cannot be entirely excluded, it is improbable that adult animals over two years old, which tested negative via qPCR and ELISA at two intervals (three months apart), were unrecognized cases. The near-complete alignment of BLV(-) reads to the bovine genome confirms their bovine origin, while a small subset of reads mapped exclusively to viral miRNAs. Therefore, it suggests that the reads aligning to BLV- and BFV-derived miRNAs in BLV(-) samples are likely bona fide and not the result of cross-mapping or artifacts (data not shown). Moreover, sample mislabeling appears to be unlikely, if such an issue had occurred, it would expect to observe expression profiles of viral miRNAs in BLV(+) samples that mirrored those of BLV(-). However, our data did not show such patterns. The miRNA expression profiles in BLV(-) samples were not consistent with those from BLV(+) samples, further arguing against sample misidentification or cross-contamination. The potential for BLV- or BFV-miRNAs to function as xeno-miRs and be transmitted from infected to uninfected animals remains a question for future research.

Notably, the expression profiles of BLV(+) / BFV-miRNAs(+) and BLV(-) samples distinctly differentiate the two groups of cows groups, as shown in the PCA plot. This indicates a shift in the host miRNA expression profile between them.

Among the significant differentially expressed bovine miRNAs, bta-miR-375 was identified, which has been previously reported to be associated with BLV infection in cattle (85; 95; 98), and suggested it as an early biomarker for diagnosing enzootic bovine leukosis (EBL). Moreover, its levels effectively distinguished EBL-affected cattle from asymptomatic cattle with high sensitivity and specificity (99).

In a similar manner, bta-miR-133a was found to be differentially expressed in the serum of BLV-seropositive cows compared to seronegative cows (98). The other significantly differentially expressed miRNAs (bta-miR-677, bta-miR-95, bta-miR-9-5p, bta-miR-3613a, and bta-miR-1) have not been previously reported in relation to BLV and/or BFV infections.

To date, efforts to assign biological functions to BLV- and BFV-derived miRNAs have focused on predicting potential target genes for specific BLV- and BFV-miRNAs, in addition to selecting candidate target genes for functional assays (21; 41; 44; 45; 83; 84; 85). In this study, we evaluated the functional

interaction (protein-protein interaction network) of potential target genes of BLV-miRNAs, while also considering target genes of BFV-miRNAs and differentially expressed bovine-miRNAs.

It has been demonstrated that BLV-miRNAs are crucial in promoting disease progression in cattle (83; 100). Additionally, BLV fails to induce leukemia/lymphoma in sheeps (oncogenicity suppressed) challenged with an isogenic BLV provirus lacking the miRNA genomic region.

The functional annotation of the proteins within hub C1 revealed that immune system-related GO BP terms, such as "*Cytokine-mediated signaling pathway*", "*Positive regulation of leukocyte chemotaxis*", "*Regulation of leukocyte proliferation*", "*Positive regulation of T cell activation*", "*Regulation of leukocyte apoptotic process*", "*Regulation of interferon-gamma production*", were significant overrepresented, along with the KEGG and Reactome terms: "*Cytokine-cytokine receptor interaction*", "*Viral protein interaction with cytokine and cytokine receptor*", "*Cytokine signaling in immune system*". The Figure 5 A) showed the enrichment graph connecting gene target to BP GO terms. It is widely accepted that BLV infection changes the cytokines expression patterns and alters how the immune system produces cytokines in response to BLV antigen stimulation (101; 102). Particularly, BLV disease progression would be related to the suppression of the cell-mediated immune response (103). For example, Interleukin-10 (IL-10), a suppressor and anti-inflammatory immune response cytokine, is over expressed in cows with persistent lymphocytosis (104), which can inhibit cytokine production by Th1 cells (for example, IL-2, IL-12 and gamma interferon) (104; 105) influencing the B-cell proliferation and differentiation (104; 106).

In turn, the analysis of overrepresented metabolic pathways for the complete potential target gene set identified "*Pathway in cancer*" as one of the significant KEGG pathways. This pathway involves a series of cellular signaling pathways that activate crucial hallmarks of tumorigenesis, including tissue invasion and metastasis, evading apoptosis, genomic instability, cell proliferation, genomic damage, and insensitivity to anti-growth signals (107). The overrepresented GO BP terms for the biological function hub C2 included terms associated with cellular processes that, when disrupted, could be linked to tumor development events. These terms included "*Transmembrane receptor protein tyrosine kinase signaling pathway*", "*Vascular endothelial growth factor signaling pathway*", "*ERBB2-EGFR signaling pathway*", "*Positive regulation of MAP kinase activity*", "*Hemopoiesis*", "*Negative regulation of apoptotic process*",

among others. Interestingly, other overrepresented KEGG terms in C2 included the "*MAPK signaling pathway*", "*JAK-STAT signaling pathway*", "*HIF-1 signaling pathway*", "*Regulation of actin cytoskeleton*" and Reactome terms such as "*PI3K/AKT Signaling*" and "*Signaling by Receptor Tyrosine Kinases*". This signaling pathways are amplified and propagated intracellularly by various kinases, ultimately affecting how transcription factors and histone-modifying complexes control downstream gene expression (108). In this context, a crucial signaling cascade most altered in human cancers is the mitogen-activated protein kinase (MAPK) pathway, which includes the RAS–RAF–MAPK kinase (MEK)–extracellular signal-regulated kinase (ERK) pathway (109; 110). Using the ovine BLV pathogenesis model, sheeps were experimentally challenged with an isogenic BLV-miRNA deletion mutant, and global transcriptome analysis revealed that BLV-miRNAs primarily promote the proliferation of BLV-infected B-cells by inhibiting immune response and cell signaling pathways (100). In turn, in a reporter assay, the FBJ murine osteosarcoma viral oncogene homolog (*FOS*) was identified as a direct target of BLV-miRNAs. The *FOS* gene is a component of the activator protein-1 (AP-1) complex, which is involved in the primary response to B-cell receptor signaling and is frequently downregulated in many cancers, including breast carcinomas (83; 111).

Additionally, enriched GO BP terms across C3 included "*Histone modification*", "*Chromatin remodeling*", and "*Histone deacetylation*", “*Negative regulation of transcription by RNA polymerase II*”, ”*Regulation of apoptotic signaling pathway*”, among others; as well as the Reactome terms "*Regulation of TP53 Activity through Acetylation*" and "*Chromatin modifying enzymes*". The transcription factor *TP53*, a tumor suppressor activated by DNA damage, plays a critical role in maintaining genomic integrity (112). The expression of two transcription factors, B-lymphocyte-induced maturation protein 1 (*BLIMP1*) and B-cell lymphoma 6 (*BCL6*), is negatively correlated with BLV-miRNA expression in BLV(+) cows. These transcription factors play a pivotal role regulating B-cell differentiation, antibody affinity and T-cells immune function. Particularly, an important function of *BCL6* is to enable GC B-cells to proliferate in response to T-cell antigens by specifically repressing gene expression related to DNA damage sensing. This repression allows for the tolerance of DNA breaks induced during immunoglobulin class rearrangement and somatic hypermutation (84; 113; 114).

The functional role of BFV-miRNAs remains poorly investigated. Predicted gene targets for bfv-miR-BF2-5p were Ankyrin repeat domain-containing protein (*ANKRD17*) and Bax-interacting factor 1 (*BIF1*) (41). *BIF1* plays a key role in activating the pro-apoptotic Bax protein in the intrinsic apoptosis pathway as well as in autophagy and autophagosome formation, thus acting as a tumor suppressor (115; 116). *ANKRD17,* on the other hand, is involved in DNA replication and cell cycle progression. It also interacts with genes that are responsible for sensing viral RNAs and trigger immune responses (117; 118).

Notably, although target genes of bovine, BLV, and BFV miRNAs do not overlap, functional analysis revealed convergence on similar cellular processes, implying coordinated regulatory interactions (Figure 5).

Regarding the differentially expressed BTA-miRNAs, miR-1, miR-133a, and miR-375 are recognized as tumor suppressors and are downregulated in various types of cancer, exerting their effects through distinct mechanisms (119; 120). For instance, miR-1 interacts with the proto-oncogene B-cell lymphoma 2 (*BCL-2*), an anti-apoptotic gene. Overexpression of miR-1 inhibits cell proliferation, migration, and invasion while promoting apoptosis in breast cancer (121). Similarly, miR-133a modulates biological processes such as proliferation, apoptosis, and autophagy (120). On the other hand, miR-375 is significantly downregulated in several cancers and considered a biomarker of poor prognosis (122; 123; 124; 125), but it is overexpressed in breast cancer (126). Similarly, miR-95-3p and miR-9-3p act as prognostic markers, promoting the progression of cervical and breast cancers, respectively (127; 128).

Conversely, the differentially expressed bovine miRNA bta-miR-677 enhances the production of type I interferons (IFN-I) and interferon-stimulated genes (ISGs) (129). Similarly, inhibiting miR-3613-3p decreases the expression of IFN-α and IFN-β, thereby affecting the anti-hepatitis B activity of interferons (130). Moreover, miR-3613-3p has been recognized as a tumor suppressor, with its deletion associated with poor prognosis in estrogen receptor-positive breast cancer patients (131).

## Conclusion

In this study, we report for the first time the co-expression of seven miRNAs derived from BLV and three from BFV in cattle naturally infected with BLV. Several bovine BTA-miRNAs were found to be

differentially expressed (DE) between cows with BLV high proviral load (PVL) and non-infected cows. Among them, bta-miR-375 was previously identified as a potential early biomarker for the progression of enzootic bovine leukosis, and this study further emphasizes its potential utility in identifying high PVL cows alongside other candidate miRNAs.

The functional analysis of protein-protein interaction networks involving BLV-, BFV-, and BTA-DE miRNAs-targeted genes identified key metabolic pathways that potentially underlie tumorigenesis and immune response modulation, including cellular signaling pathways, regulation of T cell activation, apoptosis, chromatin remodeling, and cytoskeleton regulation. Moreover, miRNA targets from both host and viral origins would act synergistically to influence cellular processes. The co-expression of miRNAs derived from BLV and BFV raises concerns about whether their interaction may exacerbate disease pathogenesis or facilitate the dissemination of BFV in light of the zoonotic potential that BFV presents. Ultimately, the identified miRNAs and associated metabolic pathways offer promising opportunities for developing diagnostic tools and therapeutic strategies aimed at controlling viral persistence and tumorigenesis in cattle.

## Declarations

## Competing interests

The authors declare that they have no competing interests.

## Funding

The present study was partially supported by the Instituto Nacional de Tecnología Agropecuaria (INTA, Argentina) projects 2023-2017-PD-I113 and 2023-2027-PD-I114, the Fondo para la Investigación Científica y Tecnológica (FONCyT) PICT-2017-0262, and by the Consejo Nacional de Investigaciones Científicas y Técnicas (CONICET, Argentina) PIP 2021- 2023-11220200101106CO01

## Authors' contributions

Conceptualization: DDG, CM, JPJ, HAC.

Data curation: HAC.

Formal analysis: MIP, HAC.

Funding acquisition: CM, JPJ, HAC

Investigation: MIP, GSA, CP, DDG, KGT, CM, JPJ, HAC.

Methodology: HAC.

Visualization: HAC.

Writing – original draft: HAC.

Writing – review & editing: MIP, GSA, CP, DDG, KGT, CM, JPJ, HAC.

Roles as defined by: CRediT (contributor role taxonomy)

## Availability of data

Raw small sequencing reads are available in the NCBI Sequence Read Archive (SRA) under BioProject accession number PRJNA1219522.

## Acknowledgments

We would like to thank Dr. Andrea Puebla and Pablo Vera from the Genomic Unit (IABIMO, INTA-CONICET) for their technical assistance with the small RNA next-generation sequencing assay.

## References

1. Ruivinho C, Gama-Carvalho M. 20 June 2023. Small non-coding RNAs encoded by RNA viruses: old controversies and new lessons from the COVID-19 pandemic. Front Genet. 21;14:1216890. https://doi.org/10.3389/fgene.2023.1216890.

2. Samols MA, Hu J, Skalsky RL, Renne R. 1 July 2005. Cloning and identification of a microRNA cluster within the latency-associated region of Kaposi's sarcoma-associated herpesvirus. J Virol. 79:9301-5. https://doi.org/10.1128/JVI.79.14.9301-9305.2005.

3. Sullivan CS, Ganem D. 7 October 2005. MicroRNAs and viral infection. Mol Cell.;20:3-7. https://doi.org/10.1016/j.molcel.2005.09.012.

4. Grundhoff A, Sullivan CS. 15 March 2011. Virus-encoded microRNAs. Virology. 15;411:325-43. https://doi.org/10.1016/j.virol.2011.01.002.

5. Guo YE, Steitz JA. 21 July 2014. Virus meets host microRNA: the destroyer, the booster, the hijacker. Mol Cell Biol. 34(20):3780-7. https://doi.org/10.1128/MCB.00871-14.

6. Bartel DP. 23 January 2004 MicroRNAs: genomics, biogenesis, mechanism, and function. Cell. 116(2):281-97. https://doi.org/10.1016/s0092-8674(04)00045-5.

7. Kim VN. 1 May 2005. MicroRNA biogenesis: coordinated cropping and dicing. Nat Rev Mol Cell Biol. 6(5):376-85. https://doi.org/10.1038/nrm1644.

8. Bartel DP. 23 January 2009. MicroRNAs: target recognition and regulatory functions. Cell. 136(2):215-33. https://doi.org/10.1016/j.cell.2009.01.002.

9. He L, Hannon GJ. 1 July 2004. MicroRNAs: small RNAs with a big role in gene regulation. Nat Rev Genet. 5(7):522-31. https://doi.org/10.1038/nrg1379.

10. Friedman RC, Farh KK, Burge CB, Bartel DP. January 2009. Most mammalian mRNAs are conserved targets of microRNAs. Genome Res. 19(1):92-105. https://doi.org/10.1101/gr.082701.108.
11. Bartel DP. 22 March 2018. Metazoan MicroRNAs. Cell. 173(1):20-51. https://doi.org/10.1016/j.cell.2018.03.006.
12. Girardi E, López P, Pfeffer S. 1 October 2018 On the Importance of Host MicroRNAs During Viral Infection. Front Genet. 9:439. https://doi.org/10.3389/fgene.2018.00439.
13. Skalsky RL, Cullen BR. 2010. Viruses, microRNAs, and host interactions. Annu Rev Microbiol. 64:123-41. https://doi.org/10.1146/annurev.micro.112408.134243.
14. Pfeffer S, Zavolan M, Grässer FA, Chien M, Russo JJ, Ju J, John B, Enright AJ, Marks D, Sander C, Tuschl T. 30 April 2004. Identification of virus-encoded microRNAs. Science. 304(5671):734-6. https://doi.org/10.1126/science.1096781.
15. Pfeffer S, Sewer A, Lagos-Quintana M, Sheridan R, Sander C, Grässer FA, van Dyk LF, Ho CK, Shuman S, Chien M, Russo JJ, Ju J, Randall G, Lindenbach BD, Rice CM, Simon V, Ho DD, Zavolan M, Tuschl T. 16 February 2005. Identification of microRNAs of the herpesvirus family. Nat Methods. 2(4):269-76. https://doi.org/10.1038/nmeth746.
16. Seo GJ, Fink LH, O'Hara B, Atwood WJ, Sullivan CS. 6 August 2008. Evolutionarily conserved function of a viral microRNA. J Virol. 82(20):9823-8. https://doi.org/10.1128/JVI.01144-08.
17. Ghosh Z, Mallick B, Chakrabarti J. 18 December 2008. Cellular versus viral microRNAs in host-virus interaction. Nucleic Acids Res. 37(4):1035-48. https://doi.org/10.1093/nar/gkn1004.
18. Hussain M, Torres S, Schnettler E, Funk A, Grundhoff A, Pijlman GP, Khromykh AA, Asgari S. 12 November 2011. West Nile virus encodes a microRNA-like small RNA in the 3' untranslated region which up-regulates GATA4 mRNA and facilitates virus replication in mosquito cells. Nucleic Acids Res. 40(5):2210-23. https://doi.org/10.1093/nar/gkr848.
19. Hussain M, Asgari S. 3 February 2014 MicroRNA-like viral small RNA from Dengue virus 2 autoregulates its replication in mosquito cells. Proc Natl Acad Sci US 111(7):2746-51. https://doi.org/ 10.1073/pnas.1320123111.
20. Liang H, Zhou Z, Zhang S, Zen K, Chen X, Zhang C. 29 September 2014. Identification of Ebola virus microRNAs and their putative pathological function. Sci China Life Sci. 57(10):973-81. https://doi.org/10.1007/s11427-014-4759-2.
21. Kincaid RP, Burke JM, Sullivan CS. 30 January 2012. RNA virus microRNA that mimics a B-cell oncomiR. Proc Natl Acad Sci US 109(8):3077-82. https://doi.org/10.1073/pnas.1116107109.
22. Kincaid RP, Chen Y, Cox JE, Rethwilm A, Sullivan CS. 8 April 2014. Noncanonical microRNA (miRNA) biogenesis gives rise to retroviral mimics of lymphoproliferative and immunosuppressive host miRNAs. mBio 5(2):e00074. https://doi.org/10.1128/mBio.00074-14.
23. Whisnant AW, Kehl T, Bao Q, Materniak M, Kuzmak J, Löchelt M, Cullen BR. 1 May 2014. Identification of novel, highly expressed retroviral microRNAs in cells infected by bovine foamy virus. J Virol. 88(9):4679-86. https://doi.org/10.1128/JVI.03587-13.
24. Yao Y, Smith LP, Nair V, Watson M. January 2014. An avian retrovirus uses canonical expression and processing mechanisms to generate viral microRNA. J Virol. 88(1):2-9. https://doi.org/10.1128/JVI.02921-13.
25. Teng Y, Wang Y, Zhang X, Liu W, Fan H, Yao H, Lin B, Zhu P, Yuan W, Tong Y, Cao W. 26 May 2015. Systematic Genome-wide Screening and Prediction of microRNAs in EBOV During the 2014 Ebolavirus Outbreak. Sci Rep. 5:9912. https://doi.org/10.1038/srep09912.
26. Cao W, Heit A, Hotz-Wagenblatt A, Löchelt M. 31 May 2018. Functional characterization of the bovine foamy virus miRNA expression cassette and its dumbbell-shaped pri-miRNA. Virus Genes. 54(4):550-560. https://doi.org/10.1007/s11262-018-1574-z.
27. Hashimoto-Gotoh A, Kitao K, Miyazawa T. 23 January 2020. Persistent Infection of Simian Foamy Virus Derived from the Japanese Macaque Leads to the High-Level Expression of microRNA that Resembles the miR-1 microRNA Precursor Family. Microbes Environ. 35(1):ME19130. https://doi.org/10.1264/jsme2.ME19130.
28. Aso S, Kitao K, Hashimoto-Gotoh A, Sakaguchi S, Miyazawa T. 13 November 2021. Identification of Feline Foamy Virus-derived MicroRNAs. Microbes Environ. 36(4):ME21055. https://doi.org/10.1264/jsme2.ME21055.
29. Harwig A, Das AT, Berkhout B. 23 April 2014. Retroviral microRNAs. Curr Opin Virol. 7:47-54. https://doi.org/10.1016/j.coviro.2014.03.013.
30. Aguado LC, tenOever B. 31 May 2018. RNA virus building blocks-miRNAs not included. PLoS Pathog. 14(5):e1006963. https://doi.org/10.1371/journal.ppat.1006963.

31. Vasudevan S, Tong Y, Steitz J. 21 December 2007. Switching from Repression to Activation: MicroRNAs Can Up-Regulate Translation. Science. 318, 5858:1931-1934. https://doi.org/10.1126/science.1149460.
32. Chenarboo F, Ng H, Macdonald D, Mahal L. 23 November 2022. High-Throughput Analysis Reveals miRNA Upregulating α-2,6-Sialic Acid through Direct miRNA–mRNA Interactions. ACS Cent. Sci. 8, 11, 1527–1536. https://doi.org/10.1021/acscentsci.2c00748.
33. Cullen BR. 22 January 2009. Viral and cellular messenger RNA targets of viral microRNAs. Nature. 22;457(7228):421-5. https://doi.org/10.1038/nature07757.
34. Cullen BR. 15 February 2013. MicroRNAs as mediators of viral evasion of the immune system. Nat Immunol. 14(3):205-10. https://doi.org/10.1038/ni.2537.
35. Tycowski KT, Guo YE, Lee N, Moss WN, Vallery TK, Xie M, Steitz JA. 15 March 2015. Viral noncoding RNAs: more surprises. Genes Dev. 29(6):567-84. https://doi.org/10.1101/gad.259077.115.
36. Pluta A, Jaworski JP, Douville RN. 25 September 2020. Regulation of Expression and Latency in BLV and HTLV. Viruses. 12(10):1079. https://doi.org/10.3390/v12101079.
37. Glazov EA, Horwood PF, Assavalapsakul W, Kongsuwan K, Mitchell RW, Mitter N, Mahony TJ. 1 January 2010. Characterization of microRNAs encoded by the bovine herpesvirus 1 genome. J Gen Virol. 91:32-41. https://doi.org/10.1099/vir.0.014290-0.
38. Tang Q, Wu YQ, Chen DS, Zhou Q, Chen HC, Liu ZF. 1 March 2014. Bovine herpesvirus 5 encodes a unique pattern of microRNAs compared with bovine herpesvirus 1. J Gen Virol. 95:671-678. https://doi.org/10.1099/vir.0.061093-0.
39. Jaber T, Workman A, Jones C. 21 April 2010. Small noncoding RNAs encoded within the bovine herpesvirus 1 latency-related gene can reduce steady-state levels of infected cell protein 0 (bICP0). J Virol. 84(13):6297-307. https://doi.org/10.1128/JVI.02639-09.
40. da Silva LF, Jones C. February 2012. Two microRNAs encoded within the bovine herpesvirus 1 latency-related gene promote cell survival by interacting with RIG-I and stimulating NF-κB-dependent transcription and beta interferon signaling pathways. J Virol. 86(3):1670-82. https://doi.org/10.1128/JVI.06550-11.
41. Cao W, Stricker E, Hotz-Wagenblatt A, Heit-Mondrzyk A, Pougialis G, Hugo A, Kuźmak J, Materniak-Kornas M, Löchelt M. 2 November 2020. Functional Analyses of Bovine Foamy Virus-Encoded miRNAs Reveal the Importance of a Defined miRNA for Virus Replication and Host-Virus Interaction. Viruses. 12(11):1250. https://doi.org/10.3390/v12111250.
42. Han YC, Park CY, Bhagat G, Zhang J, Wang Y, Fan JB, et al. 15 March 2010. microRNA-29a induces aberrant self-renewal capacity in hematopoietic progenitors, biased myeloid development, and acute myeloid leukemia. J Exp Med. 207: 475–489. https://doi.org/10.1084/jem.20090831.
43 Santanam U, Zanesi N, Efanov A, Costinean S, Palamarchuk A, Hagan JP, et al. 21 June 2010 Chronic lymphocytic leukemia modeled in mouse by targeted miR-29 expression. Proc Natl Acad Sci U S A. 107: 12210–12215. https://doi.org/10.1073/pnas.1007186107.
44. Rosewick N, Momont M, Durkin K, Takeda H, Caiment F, Cleuter Y, Vernin C, Mortreux F, Wattel E, Burny A, Georges M, Van den Broeke A. 23 january 2013. Deep sequencing reveals abundant noncanonical retroviral microRNAs in B-cell leukemia/lymphoma. Proc Natl Acad Sci U S A. 110(6):2306-11. https://doi.org/10.1073/pnas.1213842110.
45. Petersen MI, Carignano HA, Mongini C, Gonzalez DD, Jaworski JP. 2 February 2023. Bovine leukemia virus encoded blv-miR-b4-3p microRNA is associated with reduced expression of anti-oncogenic gene in vivo. PLoS One 18(2):e0281317. https://doi.org/10.1371/journal.pone.0281317.
46. VanLeeuwen JA, Forsythe L, Tiwari A, Chartier R. January 2005. Seroprevalence of antibodies against bovine leukemia virus, bovine viral diarrhea virus, Mycobacterium avium subspecies paratuberculosis, and Neospora caninum in dairy cattle in Saskatchewan. Can Vet J. 46:56–58.
47. VanLeeuwen JA, Tiwari A, Plaizier JC, Whiting TL. August 2006. Seroprevalences of antibodies against bovine leukemia virus, bovine viral diarrhea virus, Mycobacterium avium subspecies paratuberculosis, and Neospora caninum in beef and dairy cattle in Manitoba. Can Vet J. 47:783–786.
48. NAHMS. 2007. https://www.aphis.usda.gov/animal_health/nahms/dairy/downloads/dairy07/Dairy07_is_BLV.pdf.

49. Gutiérrez G, Carignano H, Alvarez I, Martínez C, Porta N, Politzki R, Gammella M, Lomonaco M, Fondevila N, Poli M, Trono K. 9 October 2012. Bovine leukemia virus p24 antibodies reflect blood proviral load. BMC Vet Res. 8:187. https://doi.org/10.1186/1746-6148-8-187.
50. OIE. Manual of Diagnostic Tests and Vaccines for Terrestrial Animals. 2012. 7th Ed.
51. Erskine RJ, Bartlett PC, Byrem TM, Render CL, Febvay C, Houseman JT. 27 March 2012. Using a herd profile to determine age-specific prevalence of bovine leukemia virus in Michigan dairy herds. Vet Med Int. https://doi.org/10.1155/2012/350374.
52. Bartlett PC, Norby B, Byrem TM, Parmelee A, Ledergerber JT, Erskine RJ. March 2013. Bovine leukemia virus and cow longevity in Michigan dairy herds. J Dairy Sci. 96:1591–1597. https://doi.org/10.3168/jds.2012-5930.
53. Materniak-Kornas M, Tan J, Heit-Mondrzyk A, Hotz-Wagenblatt A, Löchelt M. 21 November 2019. Bovine Foamy Virus: Shared and Unique Molecular Features In Vitro and In Vivo. Viruses. 11(12):1084. https://doi.org/10.3390/v11121084.
54. De Brun L, Mionetto M, Rodríguez F, Brandl S, Hubner S, Fischer G, Puentes R. 15 July 2023. Natural Association between Bovine Leukemia Virus and Reproductive Infectious Diseases. Acta Scientiae Veterinariae. 51:1922. https://doi.org/10.22456/1679-9216.129251
55. Méndez A, Cerón-Téllez F, Sarmiento R, Tórtora-Pérez J, Rojas-Anaya E, Álvarez H. April 2023. Presence of co-infection between bovine leukemia virus and bovine herpesvirus 1 in herds vaccinated against bovine respiratory complex. Canadian Journal of Veterinary Research. 87(2):105-109(5).
56. Oviedo-Pastrana M, Doria-Ramos M, Mattar S, Oviedo-Socarras T, Vallejo-Timarán D. 4 August 2024. Seroprevalence of bovine leukemia virus and association with bovine infectious abortion in Creole breeds from tropical grazing herds in the Colombian Caribbean. Vet World. 17(8):1715-1721. https://doi.org/10.14202/vetworld.2024.1715-1721.
57. Petersen MI, Carignano HA, Suarez Archilla G, Caffaro ME, Alvarez I, Miretti MM, Trono K. February 2021. Expression-based analysis of genes related to single nucleotide polymorphism hits associated with bovine leukemia virus proviral load in Argentinean dairy cattle. J Dairy Sci. 104(2):1993-2007. https://doi.org/10.3168/jds.2020-18924.
58. Alvarez I, Gutiérrez G, Gammella M, Martínez C, Politzki R, González C, Caviglia L, Carignano H, Fondevila N, Poli M, Trono K. May 2013. Evaluation of total white blood cell count as a marker for proviral load of bovine leukemia virus in dairy cattle from herds with a high seroprevalence of antibodies against bovine leukemia virus. Am J Vet Res.;74(5):744-9. https://doi.org/10.2460/ajvr.74.5.744.
59. Trono KG, Pérez-Filgueira DM, Duffy S, Borca MV, Carrillo C. 26 November 2001. Seroprevalence of bovine leukemia virus in dairy cattle in Argentina: comparison of sensitivity and specificity of different detection methods. Vet Microbiol. 83(3):235-48. https://doi.org/10.1016/s0378-1135(01)00420.
60. Petersen MI, Alvarez I, Trono KG, Jaworski JP. July 2018. Quantification of bovine leukemia virus proviral DNA using a low-cost real-time polymerase chain reaction. J Dairy Sci. 101(7):6366-6374. https://doi.org/10.3168/jds.2017-14253.
61. Hopkins SG, DiGiacomo RF. March 1997. Natural transmission of bovine leukemia virus in dairy and beef cattle. Vet Clin North Am Food Anim Pract. 13(1):107-28. https://doi.org/10.1016/s0749-0720(15)30367-4.
62. Smith T, Heger A, Sudbery I. March 2017. UMI-tools: modeling sequencing errors in Unique Molecular Identifiers to improve quantification accuracy. Genome Res. 27(3):491-499. https://doi.org/10.1101/gr.209601.116.
63. Martin, M. 2011. Cutadapt removes adapter sequences from high-throughput sequencing reads. EMBnet.journal. 17(1):pp10-12. https://doi.org/10.14806/ej.17.1.200.
64. Bushnell, B. 21 March 2014. BBMap: A Fast, Accurate, Splice-Aware Aligner. Berkeley: Lawrence Berkeley National Lab. Report #: LBNL-7065E. https://escholarship.org/uc/item/1h3515gn.
65. Langmead B, Salzberg SL. 4 March 2012. Fast gapped-read alignment with Bowtie 2. Nat Methods. 9(4):357-9. https://doi.org/10.1038/nmeth.1923.
66. Liu D. 16 December 2019. Algorithms for efficiently collapsing reads with Unique Molecular Identifiers. PeerJ. 7:e8275. https://doi.org/10.7717/peerj.8275.
67. Kozomara A, Birgaoanu M, Griffiths-Jones S. 8 January 2019. miRBase: from microRNA sequences to function. Nucleic Acids Res. 47(D1):D155-D162. https://doi.org/10.1093/nar/gky1141.

68. Friedländer M, Mackowiak S, Li N, Chen W, Rajewsky N. January 2012. miRDeep2 identifica con precisión genes de microARN conocidos y cientos de nuevos en siete clados animales, Nucleic Acids Research 40(1):37–52. https://doi.org/10.1093/nar/gkr688.
69. Love MI, Huber W, Anders S. 5 December 2014. Moderated estimation of fold change and dispersion for RNA-seq data with DESeq2. Genome Biol. 15(12):550. https://doi.org/10.1186/s13059-014-0550-8.
70. Benjamini Y, Hochberg Y. 1995. Controlling the false discovery rate: A practical and powerful approach to multiple testing. J Roy Statist Soc Ser B. 57:289–300. https://doi.org/10.1111/j.2517-6161.1995.tb02031.x.
71. R Core Team, 2024. R: A Language and Environment for Statistical Computing. Vienna, Austria.
72. Enright AJ, John B, Gaul U, Tuschl T, Sander C, Marks DS. 12 December 2003. MicroRNA targets in Drosophila. Genome Biol. 5(1):R1. https://doi.org/10.1186/gb-2003-5-1-r1.
73. Kertesz M, Iovino N, Unnerstall U, Gaul U, Segal E. 23 September 2007. The role of site accessibility in microrna target recognition. Nature genetics, 39(10):1278–1284. https://doi.org/10.1038/ng2135.
74. Krüger J, Rehmsmeier M. 1 July 2006. RNAhybrid: microRNA target prediction easy, fast and flexible. Nucleic Acids Res, 34, p.W451-4. https://doi.org/10.1093/nar/gkl243.
75. Rosen BD, Bickhart DM, Schnabel RD, Koren S, Elsik CG, Tseng E, Rowan TN, Low WY, Zimin A, Couldrey C, Hall R, Li W, Rhie A, Ghurye J, McKay SD, Thibaud-Nissen F, Hoffman J, Murdoch BM, Snelling WM, McDaneld TG, Hammond JA, Schwartz JC, Nandolo W, Hagen DE, Dreischer C, Schultheiss SJ, Schroeder SG, Phillippy AM, Cole JB, Van Tassell CP, Liu G, Smith TPL, Medrano JF. 1 March 2020. De novo assembly of the cattle reference genome with single-molecule sequencing. Gigascience. 1;9(3):giaa021. https://doi.org/10.1093/gigascience/giaa021.
76. Szklarczyk D, Gable AL, Nastou KC, Lyon D, Kirsch R, Pyysalo S, Doncheva NT, Legeay M, Fang T, Bork P, Jensen LJ, von Mering C. 8 January 2021. The STRING database in 2021: customizable protein-protein networks, and functional characterization of user-uploaded gene/measurement sets. Nucleic Acids Res. 49(D1):D605-D612. doi: 10.1093/nar/gkaa1074. Erratum in: Nucleic Acids Res. 2021 Oct 11;49(18):10800. https://doi.org/10.1093/nar/gkab835.
77. Kanehisa M, Goto S. 1 January 2000. KEGG: kyoto encyclopedia of genes and genomes. Nucleic Acids Res. 28(1):27-30. https://doi.org/10.1093/nar/28.1.27.
78. Tavazoie S, Hughes JD, Campbell MJ, Cho RJ, Church GM. July 1999. Systematic determination of genetic network architecture. Nat Genet. 22(3):281-5. https://doi.org/10.1038/10343.
79. Sayols S. 18 April 2023. rrvgo: a Bioconductor package for interpreting lists of Gene Ontology terms. MicroPubl Biol. https://doi.org/10.17912/micropub.biology.000811.
80. Mirsky ML, Olmstead CA, Da Y, Lewin HA. 1996. The prevalence of proviral bovine leukemia virus in peripheral blood mononuclear cells at two subclinical stages of infection. J Virol. 70:2178–2183. https://doi.org/10.1128/jvi.70.4.2178-2183.1996.
81. Jimba M, Takeshima S, Matoba K, Endoh D, Aida Y. 2 November 2010. BLV-CoCoMo-qPCR: quantitation of bovine leukemia virus proviral load using the CoCoMo algorithm. Retrovirology. 7:91. https://doi.org/10.1186/1742-4690-7-91.
82. Mammerickx M, Portetelle D, de Clercq K, Burny A. 1987. Experimental transmission of enzootic bovine leukosis to cattle, sheep and goats: infectious doses of blood and incubation period of the disease. Leuk Res.11:353–358. https://doi.org/10.1016/0145-2126(87)90180-9.
83. Gillet NA, Hamaidia M, de Brogniez A, Gutiérrez G, Renotte N, Reichert M, Trono K, Willems L. 28 April 2016. Bovine Leukemia Virus Small Noncoding RNAs Are Functional Elements That Regulate Replication and Contribute to Oncogenesis In Vivo. PLoS Pathog. 12(4):e1005588. https://doi.org/10.1371/journal.ppat.1005588.
84. Frie MC, Droscha CJ, Greenlick AE, Coussens PM. 15 January 2018. MicroRNAs Encoded by Bovine Leukemia Virus (BLV) Are Associated with Reduced Expression of B Cell Transcriptional Regulators in Dairy Cattle Naturally Infected with BLV. Front Vet Sci. 4:245. https://doi.org/10.3389/fvets.2017.00245.
85. Casas E, Ma H, Lippolis JD. 21 September 2020. Expression of Viral microRNAs in Serum and White Blood Cells of Cows Exposed to Bovine Leukemia Virus. Front Vet Sci. 7:536390. https://doi.org/10.3389/fvets.2020.536390.
86. Cavalcante LTF, Muniz CP, Jia H, Augusto AM, Troccoli F, Medeiros SO, Dias CGA, Switzer WM, Soares MA, Santos AF. 11 December 2018. Clinical and Molecular Features of Feline Foamy Virus and Feline Leukemia Virus Co-Infection in Naturally-Infected Cats. Viruses. 10(12):702. https://doi.org/10.3390/v10120702.

87. Alais S, Pasquier A, Jegado B, Journo C, Rua R, Gessain A, Tobaly-Tapiero J, Lacoste R, Turpin J, Mahieux R. 1 October 2018. STLV-1 co-infection is correlated with an increased SFV proviral load in the peripheral blood of SFV/STLV-1 naturally infected non-human primates. PLoS Negl Trop Dis. 12(10):e0006812. https://doi.org/10.1371/journal.pntd.0006812.

88. Amborski GF, Lo L, Seger CL. July 1989. Serological detection of multiple retroviral infections in cattle: Bovine leukemia virus, bovine syncytial virus and bovine visna virus. Vet. Microbiol. 20:247–253. https://doi.org/10.1016/0378-1135(89)90048-5.

89. Jacobs RM, Smith HE, Gregory B, Valli VE, Whetstone CA. October 1992. Detection of multiple retroviral infections in cattle and cross-reactivity of bovine immunodeficiency-like virus and human immunodeficiency virus type 1 proteins using bovine and human sera in a western blot assay. Can. J. Vet. Res. 56:353–359.

90. Materniak M., Hechler T., Löchelt M., Kuzmak J. March 2013. Similar patterns of infection with bovine foamy virus in experimentally inoculated calves and sheep. J. Virol. 87:3516–3525. https://doi.org/10.1128/JVI.02447-12

91. Romen F, Backes P, Materniak M, Sting R, Vahlenkamp TW, Riebe R, Pawlita M, Kuzmak J, Löchelt M. 20 July 2007. Serological detection systems for identification of cows shedding bovine foamy virus via milk. Virology 364:123–131. https://doi.org/10.1016/j.virol.2007.03.009.

92. Pinto-Santini DM, Stenbak CR, Linial ML. 2 December 2017. Foamy virus zoonotic infections. Retrovirology. 14:55. doi: 10.1186/s12977-017-0379-9. https://doi.org/10.1186/s12977-017-0379-9.

93. Choudhary A, Galvin TA, Williams DK, Beren J, Bryant MA, Khan AS. 6 June 2013 Influence of naturally occurring simian foamy viruses (SFVs) on SIV disease progression in the Rhesus macaque (Macaca mulatta) model. Viruses. 5(6):1414–1430. https://doi.org/10.3390/v5061414.

94. Powers JA, Chiu ES, Kraberger SJ, Roelke-Parker M, Lowery I, Erbeck K, Troyer R, Carver S, VandeWoude S. 29 August 2018. Feline leukemia virus (FELV) disease outcomes in a domestic cat breeding colony: Relationship to endogenous felv and other chronic viral infections. J. Virol. 92 https://doi.org/10.1128/JVI.00649-18.

95. Ochiai C, Miyauchi S, Kudo Y, Naruke Y, Yoneyama S, Tomita K, Dongze L, Chiba Y, Hirata TI, Ichijo T, Nagai K, Kobayashi S, Yamada S, Hikono H, Murakami K. 2021 Characterization of microRNA expression in B cells derived from Japanese black cattle naturally infected with bovine leukemia virus by deep sequencing. PLoS One. 16(9):e0256588. https://doi.org/10.1371/journal.pone.0256588.

96. Lagarias DM, Radke K. May 1989. Transcriptional activation of bovine leukemia virus in blood cells from experimentally infected, asymptomatic sheep with latent infections. J Virol. 63(5):2099-107. https://doi.org/10.1128/JVI.63.5.2099-2107.1989.

97. Radke K, Sigala T, Grossman D. May 1992. Transcription of bovine leukemia virus in peripheral blood cells obtained during early infection in vivo. Microbial Pathogenesis 12:319-331 https://doi.org/10.1016/0882-4010(92)90095-6.

98. Ma H, Lippolis JD, Casas E. 18 July 2022. Expression Profiles and Interaction of MicroRNA and Transcripts in Response to Bovine Leukemia Virus Exposure. Front Vet Sci. 9:887560. https://doi.org/10.3389/fvets.2022.887560.

99. Murakami K, Matsunaga T, Matsuzaki T, Naruke Y, Miyauchi S, Kobayashi S, Yoneyama S, Sakai Y, Ichijo T, Hirata TI, Kimura A, Chiba Y, Matsuda KI, Yamada S, Hikono H. 2024. Serum bta-miRNA-375 as a potential biomarker for the early diagnosis of enzootic bovine leukosis. PLoS One. 19(5):e0302868. https://doi.org/10.1371/journal.pone.0302868.

100. Safari R, Jacques JR, Brostaux Y, Willems L. 14 May 2020. Ablation of non-coding RNAs affects bovine leukemia virus B lymphocyte proliferation and abrogates oncogenesis. PLoS Pathog. 16(5):e1008502. https://doi.org/10.1371/journal.ppat.1008502.

101. Gillet N, Florins A, Boxus M, Burteau C, Nigro A, Vandermeers F, Balon H, Bouzar AB, Defoiche J, Burny A, Reichert M, Kettmann R, Willems L. 16 March 2007. Mechanisms of leukemogenesis induced by bovine leukemia virus: prospects for novel anti-retroviral therapies in human. Retrovirology. 4:18. https://doi.org/10.1186/1742-4690-4-18.

102. Frie MC, Coussens PM. Bovine leukemia virus: A major silent threat to proper immune responses in cattle. 15 February 2015. Vet. Imm. and Imm. 163(3-4):103-114. https://doi.org/10.1016/j.vetimm.2014.11.014.

103. Kabeya H, Ohashi K, Onuma M. July 2001. Host immune responses in the course of bovine leukemia virus infection. J Vet Med Sci. 63: 703-708. https://doi.org/10.1292/jvms.63.703.

104. Pyeon D, O'Reilly KL, Splitter GA. August 1996. Increased interleukin-10 mRNA expression in tumor-bearing or persistently lymphocytotic animals infected with bovine leukemia virus. J Virol. 70(8):5706-10. https://doi.org/10.1128/JVI.70.8.5706-5710.1996.
105. Amills M, Ramiya V, Norimine J, Olmstead CA, Lewin HA. 5 December 2002. Reduced IL-2 and IL-4 mRNA expression in CD4+ T cells from bovine leukemia virus-infected cows with persistent lymphocytosis. Virology. 304: 1-9. https://doi.org/10.1006/viro.2002.1651.
106. Yakobson B, Brenner J, Ungar-Waron H, Trainin Z. 31 July 1998. Short-termed expression of interleukin-12 during experimental BLV infection may direct disease progression to persistent lymphocytosis. Vet Immunol Immunopathol. 64: 207-218. https://doi.org/10.1016/S0165-2427(98)00136-6.
107. Weinberg, R.A. 2007. The Biology of Cancer Garland Science. Taylor & Francis Group, LLC, New York, NY.
108. Suganuma T, Workman JL. June 2013. Chromatin and signaling. Curr Opin Cell Biol. 25(3):322-6. https://doi.org/10.1016/j.ceb.2013.02.016.
109. Gimple RC, Wang X. 24 September 2019. RAS: Striking at the Core of the Oncogenic Circuitry. Front Oncol. 9:965. https://doi.org/10.3389/fonc.2019.00965.
110. Bahar ME, Kim HJ, Kim DR. 18 December 2023 Targeting the RAS/RAF/MAPK pathway for cancer therapy: from mechanism to clinical studies. Signal Transduct Target Ther. 8(1):455. https://doi.org/10.1038/s41392-023-01705-z.
111. Huo L, Rothstein TL. 1 April 1995. Receptor-specific induction of individual AP-1 components in B lymphocytes. J Immunol. 154(7):3300-9.
112. Aubrey BJ, Strasser A, Kelly GL. 2 May 2016. Tumor-Suppressor Functions of the TP53 Pathway. Cold Spring Harb Perspect Med. 6(5):a026062. https://doi.org/10.1101/cshperspect.a026062.
113. Nutt SL, Fairfax KA, Kallies A. December 2007. BLIMP1 guides the fate of effector B and T cells. Nat Rev Immunol. 7(12):923-7. https://doi.org/10.1038/nri2204.
114. Swaminathan S, Duy C, Müschen M. March 2014. BACH2-BCL6 balance regulates selection at the pre-B cell receptor checkpoint. Trends Immunol. 35(3):131-7. https://doi.org/10.1016/j.it.2013.11.002.
115. Coppola D, Khalil F, Eschrich SA, Boulware D, Yeatman T, Wang HG. 15 November 2008. Down-regulation of Bax-interacting factor-1 in colorectal adenocarcinoma. Cancer. 113(10):2665-70. https://doi.org/10.1002/cncr.23892.
116. Xu L, Wang Z, He SY, Zhang SF, Luo HJ, Zhou K, Li XF, Qiu SP, Cao KY. December 2016. Bax-interacting factor-1 inhibits cell proliferation and promotes apoptosis in prostate cancer cells. Oncol Rep. 36(6):3513-3521. https://doi.org/10.3892/or.2016.5172.
117. Deng M, Li F, Ballif BA, Li S, Chen X, Guo L, Ye X. 20 March 2009. Identification and functional analysis of a novel cyclin e/cdk2 substrate ankrd17. J Biol Chem. 284(12):7875-88. https://doi.org/10.1074/jbc.M807827200.
118. Wang Y, Tong X, Li G, Li J, Deng M, Ye X. May 2012. Ankrd17 positively regulates RIG-I-like receptor (RLR)-mediated immune signaling. Eur J Immunol. 42(5):1304-15. https://doi.org/10.1002/eji.201142125.
119. Yoshino H, Chiyomaru T, Enokida H, Kawakami K, Tatarano S, Nishiyama K, Nohata N, Seki N, Nakagawa M. 1 March 2011. The tumour-suppressive function of miR-1 and miR-133a targeting TAGLN2 in bladder cancer. Br J Cancer. 104(5):808-18. https://doi.org/10.1038/bjc.2011.23.
120. Hua YT, Xu WX, Li H, Xia M. 1 January 2021. Emerging roles of MiR-133a in human cancers. J Cancer. 12(1):198-206. https://doi.org/10.7150/jca.48769.
121. Peng J, Yuan C, Wu Z, Wang Y, Yin W, Lin Y, Zhou L, Lu J. 4 May 2020. Upregulation of microRNA 1 inhibits proliferation and metastasis of breast cancer. Mol Med Rep. 22(1):454-464. https://doi.org/10.3892/mmr.2020.11111.
122. Mathé EA, Nguyen GH, Bowman ED, Zhao Y, Budhu A, Schetter AJ, Braun R, Reimers M, Kumamoto K, Hughes D, Altorki NK, Casson AG, Liu CG, Wang XW, Yanaihara N, Hagiwara N, Dannenberg AJ, Miyashita M, Croce CM, Harris CC. 2009. MicroRNA expression in squamous cell carcinoma and adenocarcinoma of the esophagus: associations with survival. Clin Cancer Res. 15(19):6192-200. https://doi.org/10.1158/1078-0432.CCR-09-1467.
123. Avissar M, Christensen BC, Kelsey KT, Marsit CJ. 15 April 2009. MicroRNA expression ratio is predictive of head and neck squamous cell carcinoma. Clin Cancer Res. 15(8):2850-5. https://doi.org/10.1158/1078-0432.CCR-08-3131.

124. Yan J, She Q, Shen X, Zhang Y, Liu B, Zhang G. 13 November 2017. Potential Role of MicroRNA-375 as Biomarker in Human Cancers Detection: A Meta-Analysis. Biomed Res Int. 2017:1875843. https://doi.org/10.1155/2017/1875843.
125. He Y, Jin J, Wang L, Hu Y, Liang D, Yang H, Liu Y, Shan B. 2017. Evaluation of miR-21 and miR-375 as prognostic biomarkers in oesophageal cancer in high-risk areas in China. Clin Exp Metastasis. 34(1):73-84. https://doi.org/10.1007/s10585-016-9828-4.
126. de Souza Rocha Simonini P, Breiling A, Gupta N, Malekpour M, Youns M, Omranipour R, Malekpour F, Volinia S, Croce CM, Najmabadi H, Diederichs S, Sahin O, Mayer D, Lyko F, Hoheisel JD, Riazalhosseini Y. 15 November 2010. Epigenetically deregulated microRNA-375 is involved in a positive feedback loop with estrogen receptor alpha in breast cancer cells. Cancer Res. 70(22):9175-84. https://doi.org/10.1158/0008-5472.CAN-10-1318.
127. Li X, Zeng Z, Wang J, Wu Y, Chen W, Zheng L, Xi T, Wang A, Lu Y. February 2020. MicroRNA-9 and breast cancer. Biomed Pharmacother. 122:109687. https://doi.org/10.1016/j.biopha.2019.109687.
128. Feng S, Lu Y, Sun L, Hao S, Liu Z, Yang F, Zhang L, Wang T, Jiang L, Zhang J, Liu S, Pang H, Wang Z, Wang H. 15 November 2022. MiR-95-3p acts as a prognostic marker and promotes cervical cancer progression by targeting VCAM1. Ann Transl Med. 10(21):1171. https://doi.org/10.21037/atm-22-5184.
129. Zhong C, Liao Z, Zhang B, Xiao L, Li J, Zhu X. August 2022. Bta-miR-677 contribute to interferon pathway affecting the proliferation of caprine parainfluenza virus type 3. Microb Pathog. 169:105642. https://doi.org/10.1016/j.micpath.2022.1056.
130. Zhao Y, Yu Y, Ye L. October 2019. MiR-3613-3p impairs IFN-induced immune response by targeting CMPK1 in chronic hepatitis B. Infect Genet Evol. 74:103919. https://doi.org/10.1016/j.meegid.2019.103919.
131. Chen C, Pan Y, Bai L, Chen H, Duan Z, Si Q, Zhu R, Chuang TH, Luo Y. 25 January 2021. MicroRNA-3613-3p functions as a tumor suppressor and represents a novel therapeutic target in breast cancer. Breast Cancer Res. 23(1):12. https://doi.org/10.1186/s13058-021-01389-9.

## Figure Legends

Figure 1. Principal component analysis of miRNAs expression matrix. Blue triangles and Red circles represent BLV(+) and BLV(-) samples, respectively. PC = principal component. PC1 and PC2, represent 62% and 17% of variance contained in the expression matrix data, respectively.

Figure 2. Volcano plot summarizing the results of the differential expression analysis of bovine miRNAs between BLV(+) and BLV(-) groups. Each circle represents a bovine miRNA. Red circles indicate miRNAs with FC < |1.5| and non-significant, while blue circles represent miRNAs with FC > |1.5| and q < 0.05 (-log(q-value) > 1.3). Viral-derived miRNAs, primarily quantified in BLV(+) samples, were excluded from the plot. Vertical dashed lines represent a |1.5| FC in miRNA expression. Horizontal dashed line represents the significance cutoff q-value = 0.05.

Figure 3. Word cloud for GO term overrepresented in target genes for Biological Process A) and Molecular Fuction B) categories.

Figure 4. Protein-protein interaction (PPI) cluster analysis. Three cluster (> 15 nodes) were identified A) Cluster 1 (C1): Nº nodes: 21 - Nº edges: 81, avg. node degree: 7.7; B) Cluster 2 (C2): Nº nodes: 20 – Nº edges: 64, avg. node degree: 6.4; C) Cluster 3 (C3): Nº nodes: 16 – Nº edges: 34, avg. node degree: 4.2. Green nodes: predicted BTA-miRNA-DE protein target; Blue nodes: predicted BFV-miRNA protein target; Red nodes: predicted BLV-miRNA protein target. Edges represent protein-protein interactions as determined by STRINGdb evidence, including: known interactions (curated databases and/or experimentally validated), predicted interactions (gene fusions, gene co-occurrence), text mining, co-expression, and protein homology.

Figure 5. Enrichment graph plot of PPI clusters. Each graph shows the relationship between the 15 top enriched BP GO terms (light pink node) and their associated gene (light blue nodes). Node size reflects the number of genes associated with each GO term (Count), and edges indicate gene-GO term associations. Genes in each graph include predicted gene targets of A) BTA-miRNA-DE, B) BLV-miRNA, and C) BFV-miRNA, respectively.

Table 1. Sample characterization and small RNA sequencing output

| Sample_ID | PR (SD)[1] | PVL | RIN | Raw Reads (n) | Reads after QC, merging and deduplication (n) | Reads mapped to bovine (%) / viral mature miRNAs[2,3] (%) | Total number of identified miRNAs (viral-miRNAs) |
|---|---|---|---|---|---|---|---|
| 5671 | 178.6(28.4) | 63,148.0 | 9.6 | 8,090,674 | 4,243,257 | 2,353,523 (96.53) / 81,744 (3.47) | 470 (10) |
| 5841 | 191.3(32.8) | 44,234.3 | 9.6 | 11,869,092 | 4,038,887 | 2,556,676 (97.08) / 74,665 (2.92) | 403 (10) |
| 6021 | 169.8(42.8) | 52,902.4 | 7.8 | 15,487,902 | 6,148,370 | 4,484,871 (92,62) / 331,369 (7.38) | 503 (10) |
| 6097 | 183.2(25.4) | 91,255.4 | 9.3 | 12,511,860 | 4,744,543 | 3,485,727 (94.31) / 198,477 (5.69) | 460 (10) |
| 5830 | <25 | - | 9.0 | 11,903,095 | 5,115,654 | 3,835,811 (99.995) / 215 (0.005) | 503 (0) |
| 6493 | <25 | - | 9.3 | 10,871,552 | 4,312,484 | 3,180,484 (99.994) / 190 (0.006) | 482 (0) |
| 6962 | <25 | - | 9.0 | 11,545,292 | 4,950,884 | 3,575,583 (99.994) / 224 (0.006) | 510 (0) |

[1]Anti-BLV enzyme-linked immunosorbent assay % of reactivity; % of reactivity values < 25.0 indicated negative samples

Abbreviatures: ID = sample identification; PR = % of reactivity; SD = standard deviation; RIN = RNA integrity number; PVL = T-3 and T0 BLV average proviral load; QC = quality control.

[2] https://www.mirbase.org/.

[3] A total of 95.7% of reads from BLV(+) samples (n = 18,402,926) and 99.9% of reads from BLV(-) samples (n = 14,378,553) aligned at least once to the Bos taurus reference genome (acc. ARS-UCD1.2). Number of reads aligned to the BLV (acc. NC_001414.1) and BFV (acc. NC_001831.1) reference genomes: 648,383 reads from all BLV(+) samples showed at least one alignment to BLV, while only 600 reads from BLV(-) cows mapped to the same genome; regarding the BFV, 138,138 reads from BLV(+) and 141 reads from BLV(-) samples had at least one aligment..

Table 2. Viral derived-miRNAs expression

| Condition | BLV(+) | | | | | BLV(-) | | | |
|---|---|---|---|---|---|---|---|---|---|
| miRNA/ID | 5671 | 5841 | 6021 | 6097 | avgexp(SD) | 5830 | 6493 | 6962 | avgexp(SD) |
| bfv-miR-BF1-5p | 8,973.2 | 719.9 | 14,813.3 | 2,872.6 | 6,844.7(6,359.3) | 15.6 | 5.8 | 15.4 | 12.3(5.6) |
| bfv-miR-BF1-3p | 12,947.2 | 1,329.6 | 15,826.4 | 2,925.9 | 8,257.3(7,204.2) | 7.1 | 11.6 | 8.6 | 9.1(2.3) |
| bfv-miR-BF2-5p | 17,694.3 | 1,735.7 | 33,383.7 | 6,868.5 | 14,920.6(13,991.2) | 0.0 | 15.4 | 17.1 | 10.8(9.4) |
| bfv-miR-BF2-3p | 2.8 | 0.0 | 6.3 | 6.2 | 3.8(3.0) | 0.0 | 0.0 | 0.0 | 0.0(0.0) |
| blv-miR-B1-5p | 0.0 | 0.0 | 0.0 | 0.0 | 0(0.0) | 0.0 | 0.0 | 0.0 | 0.0(0.0) |
| blv-miR-B1-3p | 7,556.4 | 13,726.1 | 46,243.5 | 43,198.3 | 27,681.1(19,875.4) | 28.3 | 24.1 | 24.0 | 25.5(2.5) |
| blv-miR-B2-5p | 30,941.9 | 35,856.1 | 88,113.4 | 81,320.4 | 59,057.9(29,825.4) | 60.9 | 69.4 | 71.9 | 67.4(5.7) |
| blv-miR-B2-3p | 34.2 | 47.4 | 171.3 | 197.0 | 112.5(83.6) | 0.0 | 0.0 | 0.0 | 0.0(0.0) |
| blv-miR-B3-5p | 262.0 | 371.8 | 259.8 | 344.7 | 309.6(57.3) | 0.0 | 0.0 | 0.0 | 0.0(0.0) |
| blv-miR-B3-3p | 37,074.5 | 33,573.4 | 61,540.1 | 65,060.6 | 49,312.2(16,278.9) | 39.7 | 55.9 | 53.9 | 49.8(8.8) |
| blv-miR-B4-5p | 1.4 | 0.0 | 0.0 | 1.0 | 0.6(0.7) | 0.0 | 0.0 | 0.0 | 0.0(0.0) |
| blv-miR-B4-3p | 39.9 | 69.9 | 79.8 | 70.8 | 65.1(17.4) | 0.0 | 0.0 | 0.0 | 0.0(0.0) |
| blv-miR-B5-5p | 864.3 | 972.1 | 1,218.4 | 752.0 | 951.7(199.2) | 0.7 | 1.0 | 0.9 | 0.8(0.1) |
| blv-miR-B5-3p | 0.0 | 1.2 | 0.8 | 2.1 | 1.0(0.9) | 0.0 | 0.0 | 0.0 | 0.0(0.0) |

Abbreviatures: ID = Sample ID; avgexp = normalized mean expression; SD = Standard deviation

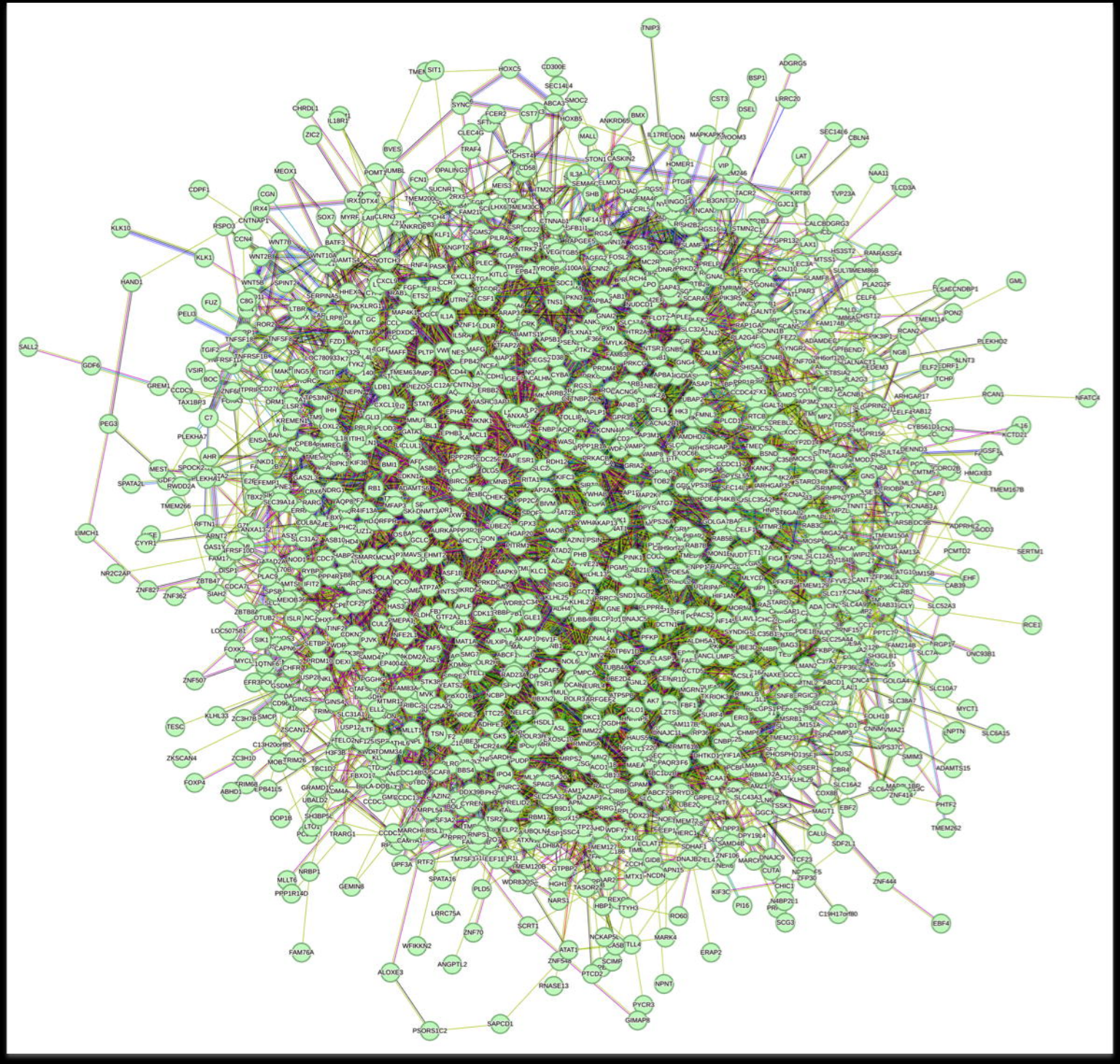

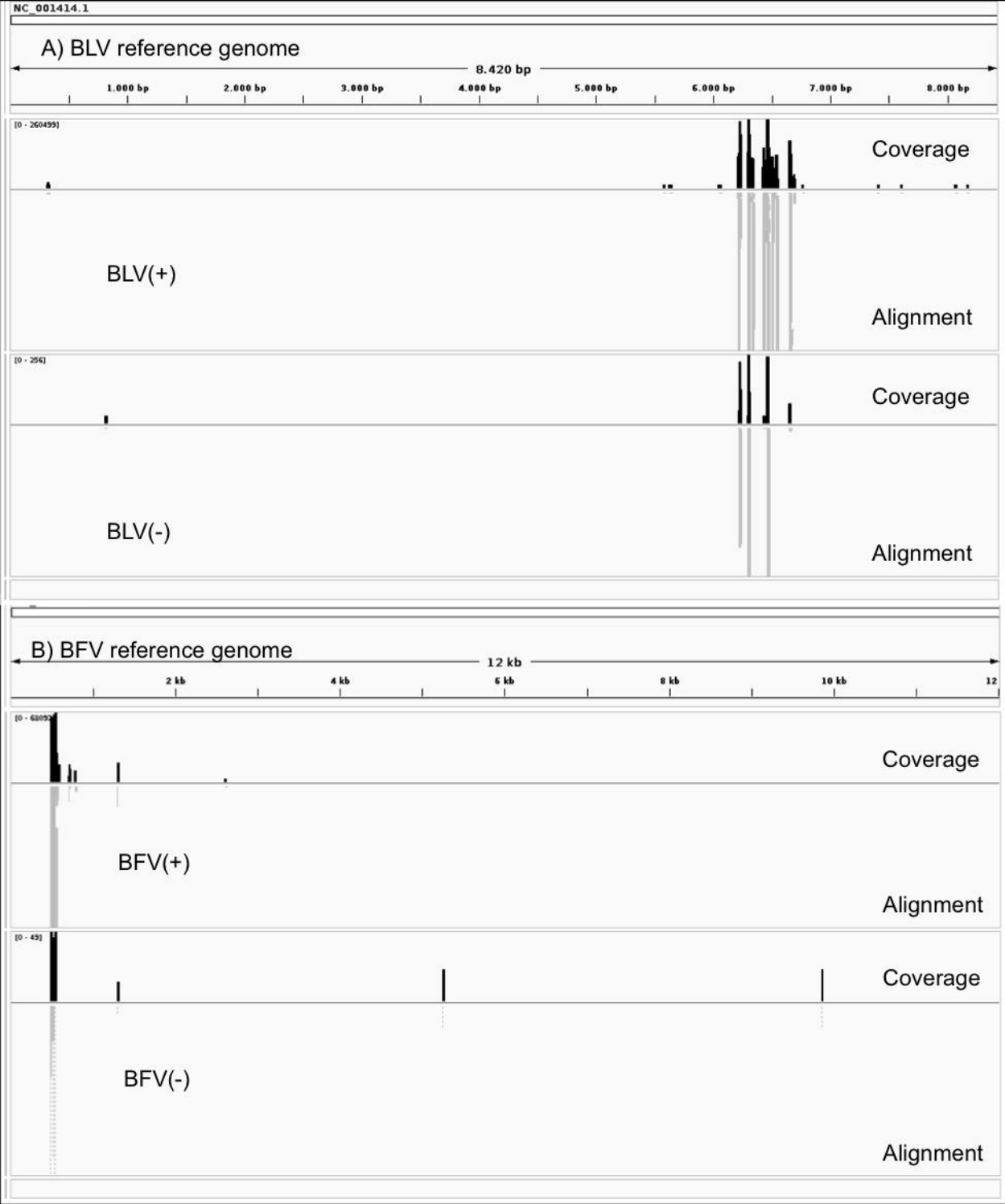
NC_001414.1
A) BLV reference genome
8.420 bp
1.000 bp
2.000 bp
3.000 bp
4.000 bp
5.000 bp
6.000 bp
7.000 bp
8.000 bp
[0 - 260495]
Coverage
BLV(+)
Alignment
[0 - 256]
Coverage
BLV(-)
Alignment
B) BFV reference genome
12 kb
2 kb
4 kb
6 kb
8 kb
10 kb
12
Coverage
BFV(+)
Alignment
[0 - 45]
Coverage
BFV(-)
Alignment

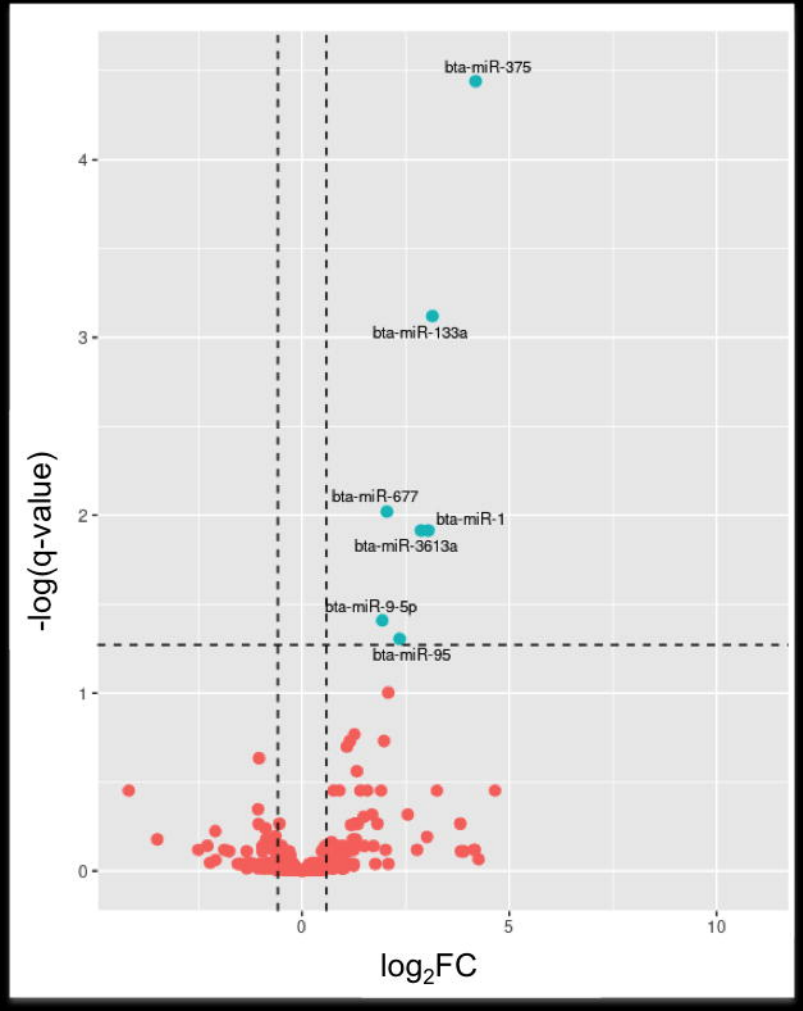
bta-miR-375
bta-miR-133a
bta-miR-677
bta-miR-1
bta-miR-3613a
bta-miR-9-5p
bta-miR-95
-log(q-value)
4
3
2
1
0
0
5
10
log2FC

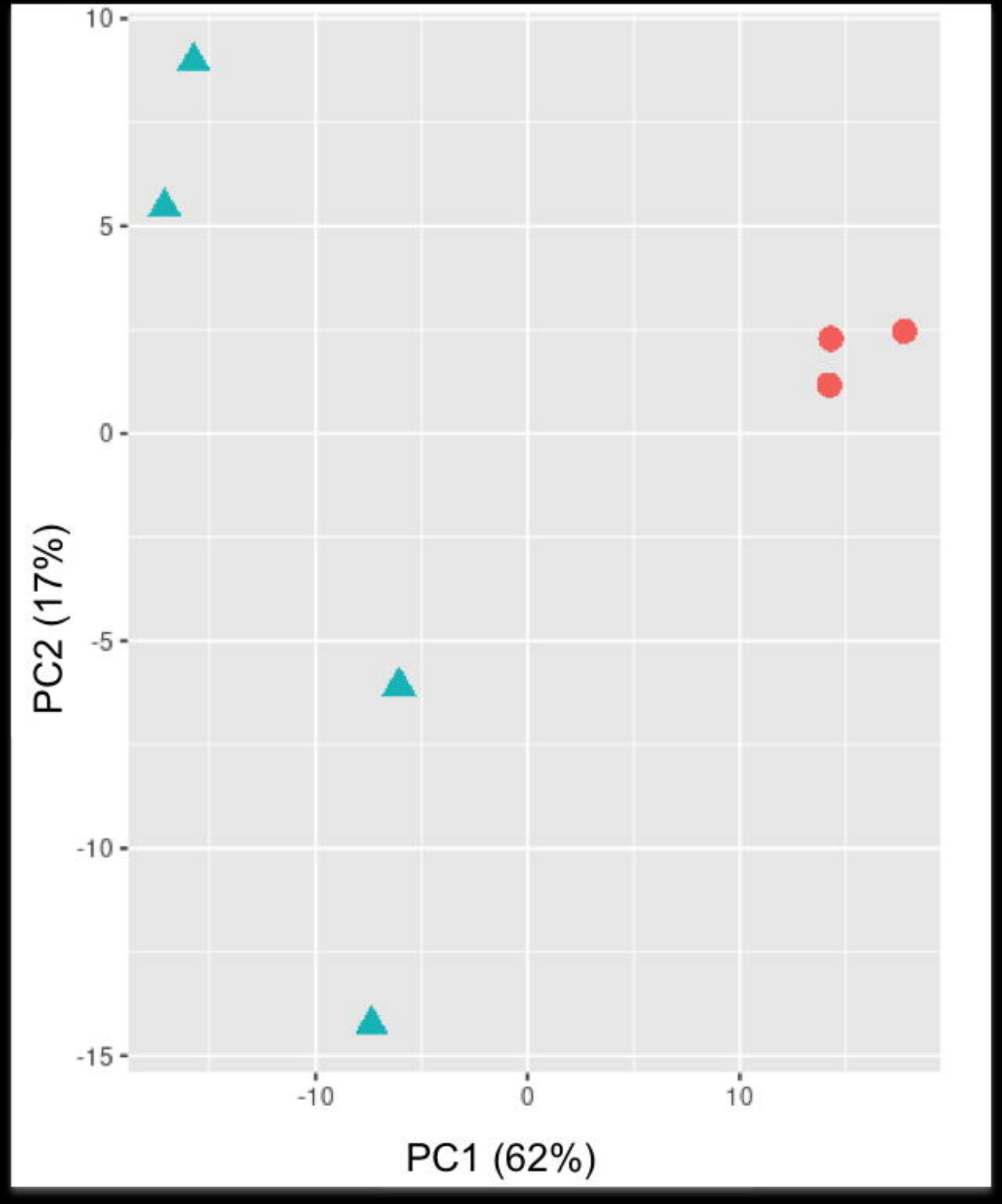
10
5
0
-5
-10
-15
PC2 (17%)
-10
0
10
PC1 (62%)

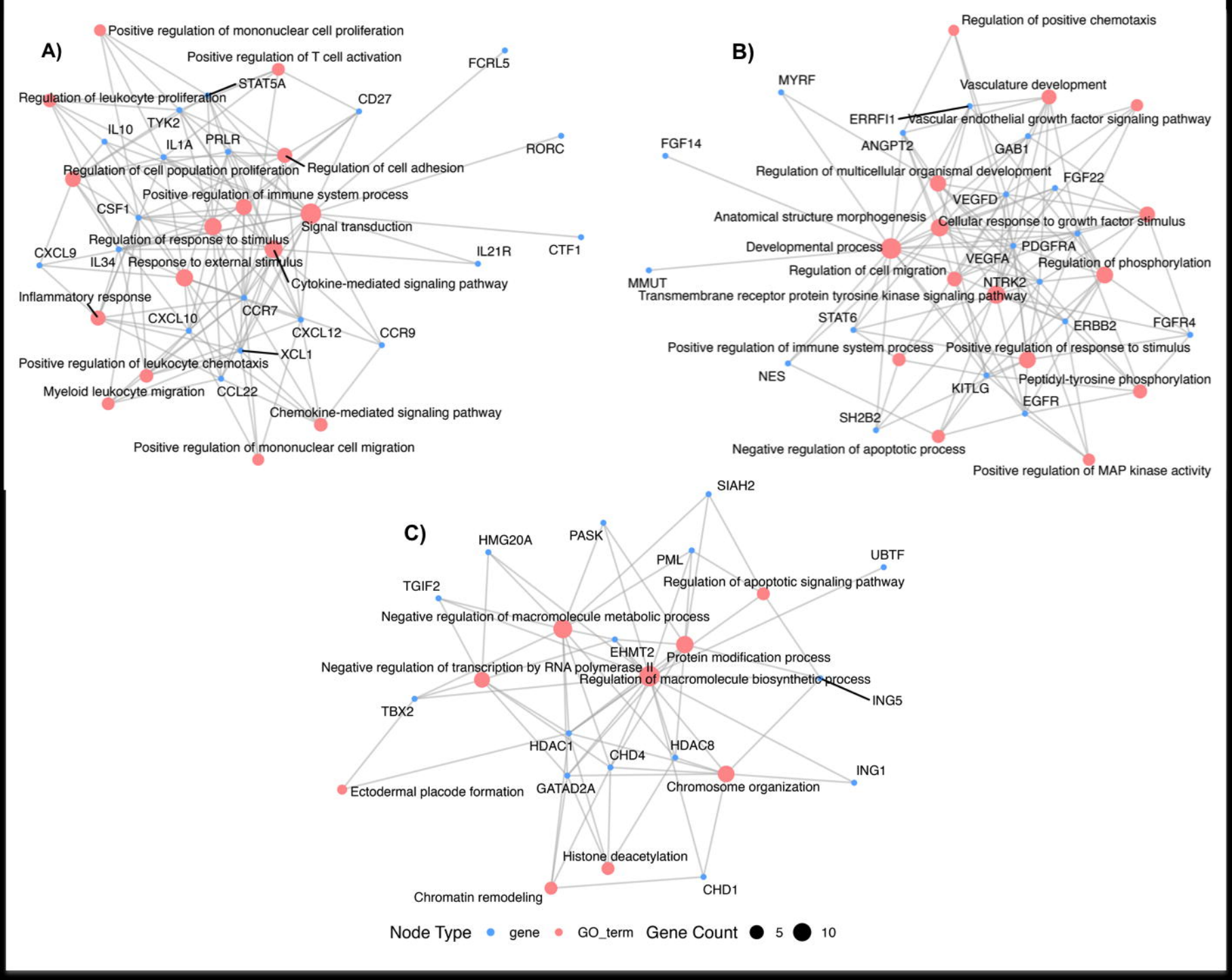
A)
Positive regulation of mononuclear cell proliferation
Positive regulation of T cell activation
FCRL5
STAT5A
Regulation of leukocyte proliferation
CD27
TYK2
IL10
IL1A
PRLR
RORC
Regulation of cell population proliferation
Regulation of cell adhesion
Positive regulation of immune system process
CSF1
Signal transduction
Regulation of response to stimulus
CXCL9
IL34
Response to external stimulus
IL21R
CTF1
Cytokine-mediated signaling pathway
Inflammatory response
CCR7
CXCL10
CXCL12
CCR9
XCL1
Positive regulation of leukocyte chemotaxis
Myeloid leukocyte migration
CCL22
Chemokine-mediated signaling pathway
Positive regulation of mononuclear cell migration
B)
Regulation of positive chemotaxis
MYRF
Vasculature development
ERRFI1
Vascular endothelial growth factor signaling pathway
FGF14
ANGPT2
GAB1
Regulation of multicellular organismal development
FGF22
VEGFD
Anatomical structure morphogenesis
Cellular response to growth factor stimulus
Developmental process
PDGFRA
VEGFA
Regulation of phosphorylation
Regulation of cell migration
MMUT
NTRK2
Transmembrane receptor protein tyrosine kinase signaling pathway
STAT6
ERBB2
FGFR4
Positive regulation of immune system process
Positive regulation of response to stimulus
NES
Peptidyl-tyrosine phosphorylation
KITLG
EGFR
SH2B2
Negative regulation of apoptotic process
Positive regulation of MAP kinase activity
C)
SIAH2
HMG20A
PASK
PML
UBTF
Regulation of apoptotic signaling pathway
TGIF2
Negative regulation of macromolecule metabolic process
EHMT2
Protein modification process
Negative regulation of transcription by RNA polymerase II
Regulation of macromolecule biosynthetic process
ING5
TBX2
HDAC1
HDAC8
CHD4
ING1
Ectodermal placode formation
GATAD2A
Chromosome organization
Histone deacetylation
Chromatin remodeling
CHD1
Node Type
gene
GO_term
Gene Count
5
10

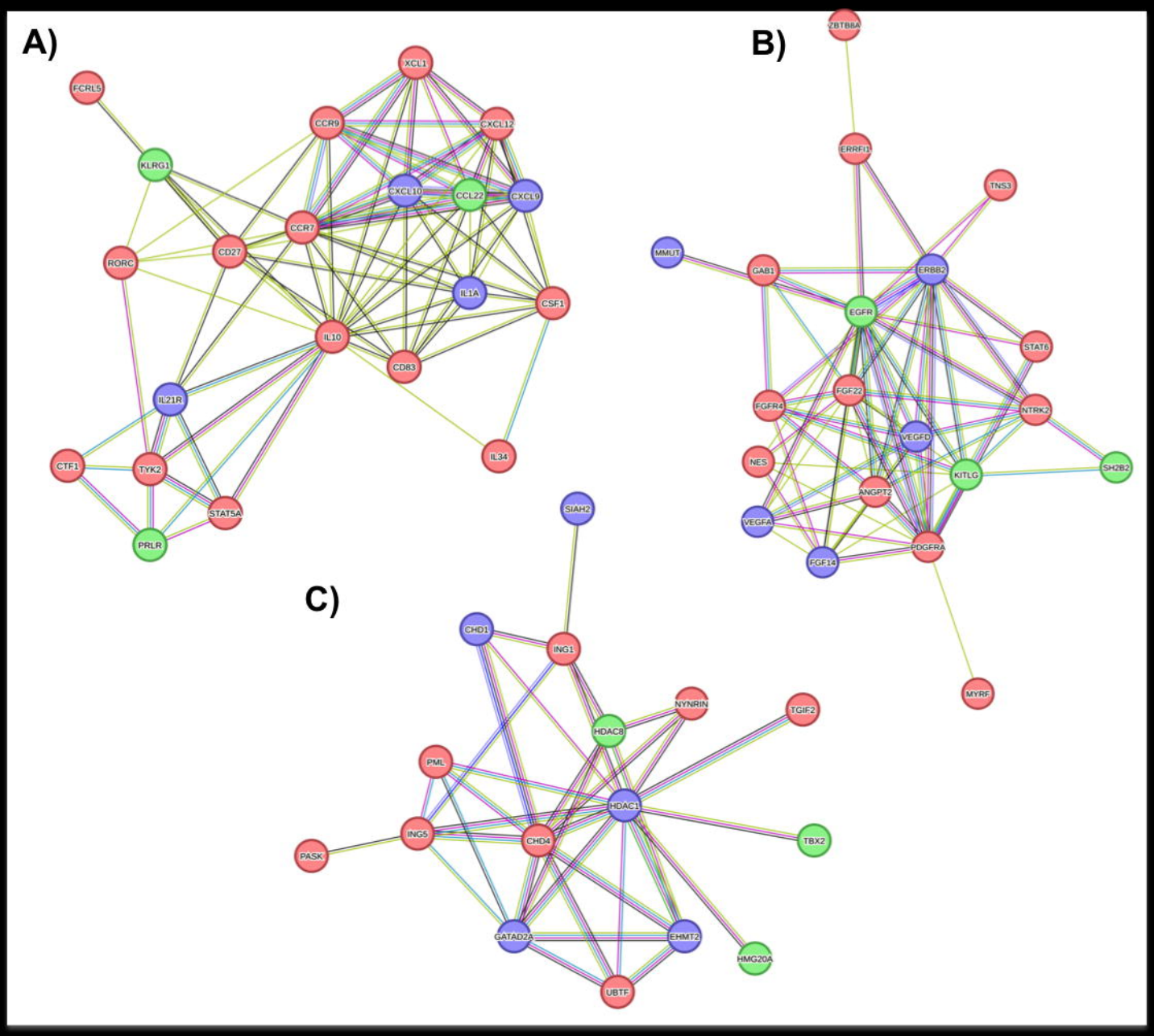
A)
FCRL5
XCL1
CCR9
CXCL12
KLRG1
CXCL10
CCL22
CXCL9
CCR7
CD27
RORC
IL1A
CSF1
IL10
CD83
IL21R
IL34
CTF1
TYK2
STAT5A
PRLR
B)
ZBTB8A
ERRFI1
TNS3
MMUT
GAB1
ERBB2
EGFR
STAT6
FGF22
FGFR4
NTRK2
VEGFD
NES
KITLG
SH2B2
ANGPT2
VEGFA
PDGFRA
FGF14
MYRF
C)
SIAH2
CHD1
ING1
NYNRIN
TGIF2
HDAC8
PML
HDAC1
ING5
CHD4
TBX2
PASK
GATAD2A
EHMT2
HMG20A
UBTF

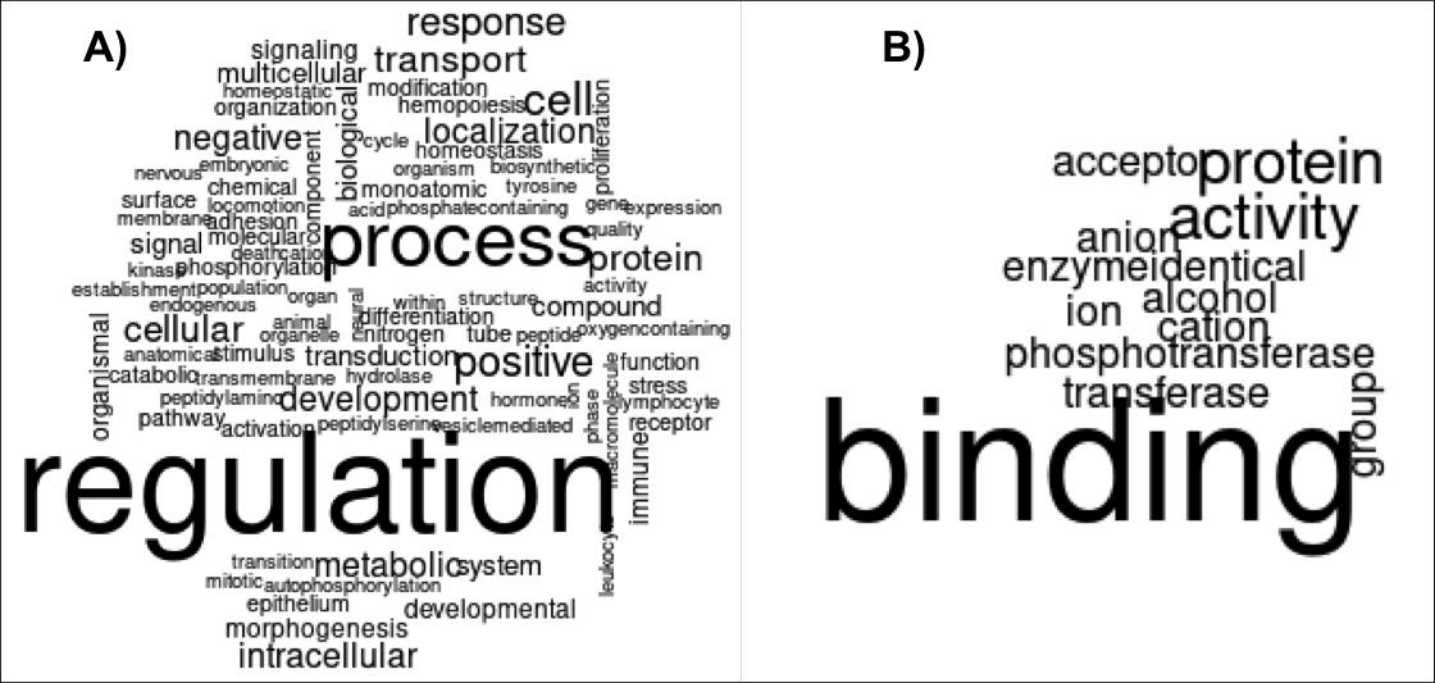
A)
response
signaling
transport
multicellular
homeostatic
modification
organization
hemopoiesis
cell
negative
localization
cycle
homeostasis
nervous
embryonic
organism
biosynthetic
chemical
monoatomic
tyrosine
surface
locomotion
acid
phosphatecontaining
gene
expression
membrane
adhesion
molecular
quality
signal
deathcation
process
protein
kinase
phosphorylation
activity
establishment
population
organ
within
structure
compound
endogenous
differentiation
animal
organelle
nitrogen
tube
peptide
oxygencontaining
cellular
anatomical
stimulus
transduction
positive
function
catabolic
transmembrane
hydrolase
stress
peptidylamino
development
hormone
lymphocyte
pathway
activation
peptidylserine
vesiclemediated
receptor
organismal
regulation
immune
transition
metabolic
system
mitotic
autophosphorylation
epithelium
developmental
morphogenesis
intracellular
B)
accepto
protein
activity
anion
enzymeidentical
ion
alcohol
cation
phosphotransferase
transferase
binding
group

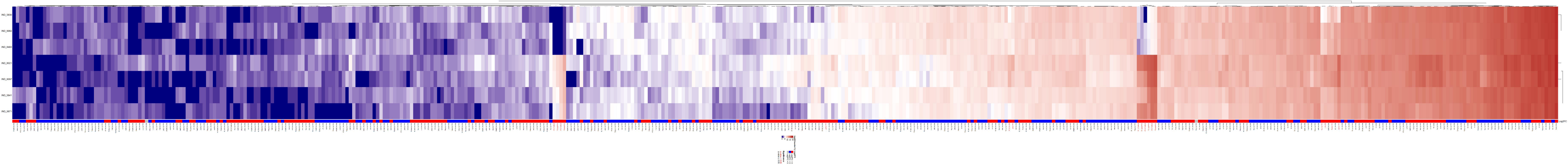
NO_SK9
NO_SK8
NO_SK5
NO_SK3
NO_SK0
NO_SK1
NO_SK7
Cluster 1
Cluster 2
log2FC
Up
Down
Other
Cluster 1
Cluster 2
Cluster 3
Cluster 4
Cluster 5
Cluster 6
Cluster 7
Cluster 8
Cluster 9
Cluster 10
Cluster 11
Cluster 12
Cluster 13
Cluster 14
Cluster 15
Cluster 16
Cluster 17
Cluster 18
Cluster 19
Cluster 20
Cluster